

# Toward Sustainable Vertical Farming: Impacts of Environmental Factors and Energy Mix on Performance and Costs

Francesco Ceccanti<sup>1\*</sup>, Aldo Bischi<sup>1</sup>, Umberto Desideri<sup>1</sup>, Andrea Baccioli<sup>1</sup>

<sup>1</sup> Department of Energy, System, Territory and Construction Engineering  
Università di Pisa, Pisa, Italy

\*Corresponding Author: [francesco.ceccanti@phd.unipi.it](mailto:francesco.ceccanti@phd.unipi.it) (F. Ceccanti)

## Abstract

The increasing interest in vertical farming arises from its ability to ensure consistent, high-quality, and pest-free vegetable production while supporting synergies with energy systems and urban development. Accordingly, standardized design and operation guidelines are essential to improve energy efficiency and lower costs. This study analyzes the production performance and energy consumption of a vertical farming system, assessing its efficiency, sustainability, and economic viability. A total of 162 scenarios were evaluated by combining three levels of temperature, photosynthetic photon flux density (PPFD), and CO<sub>2</sub> concentration across three distinct climatic zones, namely Norway, China, and Dubai, which also differ from a socio-environmental viewpoint. Two insulation thicknesses were also tested in each scenario. Results indicate that due to the heating, ventilation, and air conditioning and dehumidification (HVACD) system, neither the insulation layer nor the external climate significantly influences crop productivity. PPFD proved to be the dominant factor in crop growth (correlation: 0.85), followed by CO<sub>2</sub> (0.36) and indoor temperature (0.22). PPFD also emerged as the primary driver of overall energy consumption (correlation: 0.73), as it affects both lighting and HVACD loads. Notably, the lowest specific energy consumption (SEC) coincided with the lowest crop productivity (55 kg m<sup>-2</sup>). The levelized cost of lettuce (LCoL), balancing productivity and energy use, identified the most cost-effective setup as 24 °C, 250 μmol m<sup>-2</sup> s<sup>-1</sup> PPFD, 1400 ppm CO<sub>2</sub>, with insulation, consistent across all climates. Ultimately, only nearly decarbonized energy systems can support vertical farming without increasing CO<sub>2</sub> emissions compared to imported lettuce.

## Keywords:

Controlled Environment Agriculture; Vertical Farming; Energy System; Energy Consumption; Economic Assessment; Correlation Analysis; Food Sustainability.

## Nomenclature

Acronyms			Subscripts	
AHU	Air Handling Unit	[−]	ahu	Air Handling Unit
CAPEX	Capital Expenditures	[\$]	air	Internal Air
CEA	Controlled Environment Agriculture	[−]	c	Crop

<b>COP</b>	Coefficient of Performance	[ $kW_{th} kW_{el}^{-1}$ ]	<b>CO<sub>2</sub></b>	Carbon Dioxide
<b>CRF</b>	Capital Recovery Factor	[−]	<b>cond</b>	Condensed/Condensation
<b>DLI</b>	Daily Light Integral	[ $\mu\text{mol m}^{-2} \text{ day}^{-1}$ ]	<b>dm</b>	Dry Matter
<b>DMC</b>	Dry Matter Content	[−]	<b>el</b>	electrical
<b>HVAC</b>	Heating, Ventilation and Air Conditioning	[−]	<b>ET</b>	Evapotranspiration
<b>HVACD</b>	Heating, Ventilation and Air Conditioning and Dehumidification	[−]	<b>env</b>	Envelope
<b>LAI</b>	Leaf Area Index	[ $m_{leaf}^2 m_{soil}^{-2}$ ]	<b>eva</b>	Evaporation
<b>LCoL</b>	Levelized Cost of Lettuce	[ $\$/kg^{-1}$ ]	<b>ext</b>	External
<b>LUE</b>	Light Use Efficiency	[ $g \mu\text{mol}^{-1}$ ]	<b>fm</b>	Fresh Matter
<b>OPEX</b>	Operational Expenditure	[ $\$/\text{year}^{-1}$ ]	<b>H/C</b>	Heating&Cooling Systems
<b>PAR</b>	Photosynthetic Active Radiation	[ $\mu\text{mol m}^{-2} s^{-1}$ ]	<b>hum</b>	Humidification System
<b>PLF</b>	Part-Load Factor	[−]	<b>HP</b>	Heat Pump
<b>PLR</b>	Part-Load Ratio	[−]	<b>in</b>	Internal
<b>PPFD</b>	Photosynthetic Photon Flux Density	[ $\mu\text{mol m}^{-2} s^{-1}$ ]	<b>ins</b>	Insulation
<b>SEC</b>	Specific Energy Consumption	[ $kWh kg^{-1}$ ]	<b>Lab</b>	Labor
<b>VF</b>	Vertical Farm	[−]	<b>Leas</b>	Leasing
<b>VPD</b>	Vapour Pressure Deficit	[ $kPa$ ]	<b>LED</b>	Lighting System
<b>WUE</b>	Water Use Efficiency	[ $g_{FM} L^{-1}$ ]	<b>n</b>	Net
<b>Symbols</b>			<b>Nom</b>	Nominal
<i>A</i>	Area	[ $m^2$ ]	<b>plant</b>	Single Lettuce Plant
<i>c</i>	Specific Cost	[ $\$/x^{-1}$ ]	<b>rad</b>	Radiative
<i>c<sub>p</sub></i>	Specific Heat Capacity	[ $J kg^{-1} K^{-1}$ ]	<b>Rep</b>	Replacement
<i>C</i>	Cost	[ $\$$ ]	<b>T</b>	Temperature-Dependent
<i>d</i>	Density	[ $kg m^{-3}$ ]	<b>tot</b>	Annual
<i>D</i>	Rank Difference	[−]	<b>wat</b>	Water
<i>DM</i>	Dry Matter	[ $g m^{-2}$ ]	<b>wir</b>	Wiring
<i>e</i>	Specific Emissions	[ $g ton^{-1} km^{-1}$ ]		
<i>F</i>	Photosynthetic Photon Efficiency	[ $\mu\text{mol J}^{-1}$ ]		
<i>f</i>	CO <sub>2</sub> factor for crop growth	[−]		
<i>FM</i>	Fresh Matter	[ $g m^{-2}$ ]		
<i>K</i>	Evapotranspiration Coefficient	[−]		
<i>i</i>	Inflation Rate	[−]		
<i>I</i>	Solar Irradiation	[ $W m^{-2}$ ]		
<i>k</i>	Light Extinction Coefficient	[−]		
<i>L</i>	Supply Distance	[ $km$ ]		
<i>M</i>	Mass	[ $kg$ ]		
<i>MW</i>	Molecular Weight of Glucose	[ $g mol^{-1}$ ]		
<i>m</i>	Mass Flow	[ $kg s^{-1}$ ]		
<i>n</i>	Number of Observations	[−]		
<i>P</i>	Electrical Power	[ $kW$ ]		
<i>Q</i>	Thermal Power	[ $kW$ ]		
<i>r</i>	Interest Rate	[−]		
<i>RAD</i>	Short-wave Radiation	[ $MJ m^{-2} day^{-1}$ ]		
<i>RF</i>	Root Factor	[−]		

$T$	Temperature	[°K]		
$t$	Time	[s]		
$u$	Air Speed	[ $m\ s^{-1}$ ]		
$U$	Thermal Transmittance	[ $W\ m^{-2}\ K^{-1}$ ]		
$V$	Volume	[ $m^3$ ]		
$\alpha$	Wall's Absorption Factor	[—]		
$\epsilon$	Wall's Emissivity Factor	[—]		
$\gamma$	Psychrometric constant	[ $kPa\ ^\circ C^{-1}$ ]		
$\rho$	Spearman Coefficient	[—]		
$\eta$	Efficiency	[—]		
$\Delta$	Slope of the Saturation Curve	[ $kPa\ ^\circ C^{-1}$ ]		
$\Delta E_{phot}$	Specific Energy Requirement of Photosynthesis Reaction	[ $J\ mol^{-1}$ ]		

## 1. Introduction

In recent years, the increasing need for sustainable food production has highlighted controlled-environment agriculture (CEA) as a modern and highly relevant solution. Vertical farms (VFs) are food production systems that use hydroponic or aeroponic methods, with crops grown in multiple layers within enclosed spaces like buildings, containers, or cells. In these systems, key growth factors such as temperature, humidity, carbon dioxide levels, and photosynthetically active radiation (PAR) are meticulously controlled to optimise crop growth [1]. The vertical farming market was valued at USD 2.14 billion in 2018, and by 2023, its value had nearly tripled, reaching approximately USD 6.20 billion. The growing global population is increasing the demand for food, expanding the market for agricultural solutions. Furthermore, vertical farming is becoming increasingly popular as it offers higher yields than traditional farming methods, making it one of the main drivers of market growth. As a result, the market is projected to grow at a compound annual growth rate (CAGR) of 20.26%, reaching a total market value of USD 33.50 billion by 2032 [2].

Within these VF systems, crops are arranged on scissor lifts, ladders, or stacked A-frames, enabling the cultivation area to be expanded vertically. As a result, vertical farming can increase yields by a factor of 10 to 100 times compared to traditional open-field farming [3], and by approximately a factor equivalent to the number of stacked shelves compared to greenhouse farming [4], all while using the same land area. Moreover, as previously mentioned, thanks to the ability to precisely control growing conditions in a VF system, its corresponding crop growth rate is significantly higher. In fact, a recent study, reported in [5], compared the light use efficiency (LUE) of vertical farming with that of traditional farming methods. The study found that the average LUE value for vertical farming was  $0.55\ g_{dw}\ mol^{-1}$ , higher than both greenhouse ( $0.39\ g_{dw}\ mol^{-1}$ ) and open-field farming ( $0.23\ g_{dw}\ mol^{-1}$ ). Furthermore, the research highlighted that the maximum measured LUE

reached  $1.63 \text{ g}_{\text{dw}} \text{ mol}^{-1}$ , approaching the theoretical maximum LUE of  $1.81 \text{ g}_{\text{dw}} \text{ mol}^{-1}$ . In support of these findings, another study [6] investigated lettuce yields in a vertical farm (VF) by varying internal temperature and photosynthetically active radiation (PAR), aiming to demonstrate the higher productivity of VFs compared to conventional vegetable production systems. Indeed, under the tested conditions, LUE values ranged from 0.8 to  $1.25 \text{ g}_{\text{dw}} \text{ mol}^{-1}$ , significantly higher than those observed in traditional farming.

In 2022, hydroponics emerged as the most widely adopted cultivation method in vertical farming. In this system, crop roots are either fully submerged in a nutrient-rich solution or supplied with nutrients through techniques such as the nutrient film technique (NFT). The popularity of hydroponics is largely attributed to its relatively low installation costs and user-friendly operation. Additionally, the absence of soil significantly reduces the risk of diseases caused by soil-borne pathogens [2]. The pest-free crops produced in vertical farms are particularly appealing to consumers concerned about pesticide exposure. Beyond these advantages, hydroponic systems are also highly efficient in terms of resource use, requiring 70–95% less water than conventional farming methods [3]. All of these advantages motivated the author to further investigate this type of vertical farming system in the present study.

Vertical farming faces two major limitations: its high energy requirements and the restricted range of crop types that can be effectively cultivated in such systems. The energy consumption of vertical farms (VFs) has been widely investigated, with reported values ranging from 3.2 to  $20 \text{ kWh kg}^{-1}$  depending on the specifications of LED lighting, HVACD systems, and indoor conditions [7]. This significant variability highlights the need for a more detailed investigation into how specific input parameters influence the overall efficiency and performance of VFs. A recent review compared the energy demand of VFs with that of closed and open greenhouses, showing that VFs consume approximately twice as much energy as closed greenhouses and about three times more than open greenhouses to produce the same amount of lettuce. Notably, around 70% of a VF's total energy use is attributed to the lighting system, while heating, ventilation, and air conditioning (HVACD) systems account for approximately 28% [3]. Given that lighting accounts for the majority of energy consumption in vertical farms, [8] provides a comparative analysis of various vegetable crops based on their photon cost per unit of dry mass. The study also evaluates the photon cost as a percentage of the estimated market price of the corresponding dry mass, in order to identify the most cost-effective plant species for vertical farming. Crops characterized by a high harvest index (HI), high water content, and relatively high market value, such as lettuce, leafy microgreens, and tomatoes, are shown to be economically viable under artificial lighting. In particular, the photon cost associated with lettuce cultivation amounted to 5% of its corresponding dry market price, which helps explain why lettuce is the most commonly selected crop in VF-related studies. In contrast, [8] demonstrates that even with 100% efficient LED systems, the cultivation of staple crops like rice and wheat in vertical farms remains economically unfeasible. The widespread

popularity of lettuce led the authors to select it as the reference crop for the VF system analyzed in detail in the present study.

Recent studies aiming to improve the specific energy consumption (SEC) of vertical farms have focused on two main aspects. The first concerns the reduction of the overall energy demand of the system, while the second focuses on optimizing internal growing conditions to enhance crop productivity and, consequently, energy efficiency.

To reduce the overall energy demand of vertical farming systems, a variety of strategies have been explored. A systematic review presented in [3] categorizes these Energy Efficiency Measures (EEMs) into three main groups: Architecture/Envelope, Distributed Generation, and HVACD systems. Notably, the review identifies photovoltaic (PV) arrays as a cost-effective energy source for CEA applications. Additionally, the implementation of passive heating and cooling strategies has been shown to reduce HVACD energy loads by up to 31%.

Moreover, integration with energy systems and urban buildings could further enhance the competitiveness of vertical farms. Indeed, the integration of VF with agrivoltaic system (VFCA) has shown a 13-fold yield increase compared to traditional closed agrivoltaics [9]. Additionally, fully photovoltaic-powered vertical farms have been assessed for spatial and energy feasibility, with required PV surface areas varying by location [10]. Ultimately, from an urban standpoint, recent studies highlight the integration of vertical farming into architecture to enhance local food production and deliver social benefits [11]. Façade-based systems have also been assessed for economic and energy feasibility compared to traditional farming [18].

As highlighted by the existing literature, interest in vertical farming is rapidly increasing partly due to its multidisciplinary potential across agriculture, economics, energy systems and urban integration. Hence, the development of best practice guidelines for the design and management of vertical farms, along with a deeper understanding of how various parameters affect VF performance, is becoming increasingly essential to minimize both energy consumption and operational costs.

Photoperiod, Daily Light Integral (DLI), light use efficiency (LUE), and the spectral composition of light are key parameters influencing crop growth, as highlighted in the systematic review by Allazo et al.[12]. In particular, LUE is significantly affected by factors such as carbon dioxide concentration ( $\text{CO}_2$ ), temperature, and photosynthetic photon flux density (PPFD). Consequently, these parameters were identified as critical and included in the proposed analysis. According to [6], the optimal photoperiod for maximizing LUE, and thereby crop yield, was identified as a 16-hour light period per day. For this reason, this photoperiod was adopted in the simulations presented in the present study. On the economic front, [13] developed a methodology to compare the total production costs of vertical farming with those of conventional agriculture across seven different U.S. states, providing a regionalized economic assessment. Although the economic comparison with traditional farming was well detailed, the assumptions regarding resource consumption and productivity in vertical farming require a more rigorous and accurate approach. More

recently, in 2024, [14] introduced an integrative study combining both agronomic and economic perspectives. This work assessed the effects of indoor temperature, DLI, and LED efficiency on crop yield, energy consumption, and the cost of lettuce production, with the analysis extended across three distinct climatic zones. The findings underline the importance of site-specific design and operation strategies to ensure the sustainability and profitability of vertical farming systems. However, in [14], neither the impact of the CO<sub>2</sub> concentration on crop growth nor the effect of the envelope's insulation layer on energy consumption was investigated. Furthermore, that study's cost analysis for lettuce considered only electricity and natural gas expenses. Ultimately, [15] conducted a carbon emissions analysis related to vertical lettuce cultivation, based on a limited case study carried out in the Netherlands.

To the best of the authors' knowledge, the scientific contribution of this study lies in providing a comprehensive and detailed analysis of both the production performance and energy consumption of a vertical farming system, with the aim of enhancing its efficiency (expressed in kWh kg<sup>-1</sup>), sustainability (expressed in kgCO<sub>2</sub> saved per year), and economic viability (expressed in \$ kg<sup>-1</sup>). To enhance the understanding of how individual input parameters influence key performance indicators, a distance correlation analysis was conducted. This approach is considered more appropriate than the Spearman correlation coefficient for capturing complex non-linear relationships. The results of the analysis were then used to develop some best practices for the design and management of a VF, tailored to different socio-environmental conditions. This study builds on the findings of [23] and incorporates all three growing parameters (temperature, photosynthetically active radiation, and CO<sub>2</sub> concentration) into an accurate energy model to assess their impact on energy consumption. The results were obtained using a dynamic model previously introduced and validated, with both simulated and experimental data, in [16]. Unlike the transient model proposed by [17], which focused solely on estimating thermal load and crop yield, the model adopted in this work enables a more comprehensive evaluation. Specifically, it accounts for thermal load, crop production, water and CO<sub>2</sub> requirements, and electricity consumption. The analysis assumes that the indoor environmental conditions are maintained by an HVACD system based on a heat pump, aligning with the electrification objectives for the CEA sector outlined in [18]. Furthermore, while [17] proposed a model in which the vertical farm is placed within a building maintained at a constant indoor temperature, the present study extends the analysis by evaluating heat transfer through the building envelope. This allows for the assessment of the VF's thermal behaviour under varying external climatic conditions. From an economic standpoint, this work also includes capital expenditures (CAPEX) and a more detailed assessment of operational expenditures (OPEX) to evaluate the cost of lettuce production, in comparison with the approach adopted in [14]. Ultimately, in addition to assessing the primary energy consumption of the vertical farming system under investigation, this study aims to quantify its overall carbon footprint by comparing it with the emissions associated with supply chains for non-locally produced fresh lettuce. The analysis is extended across

different climate zones to provide a more accurate estimation of key vertical farming performance indicators.

To provide the assessments outlined above, this study examined 162 different scenarios, considering three levels each of temperature, PPF, CO<sub>2</sub> concentration, and three distinct climatic and social zones. Additionally, to evaluate the impact of the insulation layer on energy consumption, two different insulation thicknesses were analysed for each scenario. For each scenario, total energy consumption was reported to identify the most promising configurations. Subsequently, assuming that the HVACD system was powered by heat pumps, the VF's electrical loads were calculated. Based on the energy mix and economic conditions in the studied climatic zones, the carbon footprint, primary energy consumption, and economic feasibility were assessed. Finally, through assumptions about the supply chain in these zones, the carbon footprint of vertically produced crops was compared to that of traditionally produced crops, both locally sourced and imported.

## 2. Methodology

### 2.1. Vertical Farm Agri-Energy Model

The assessments extensively discussed in the following Results section are based on the comprehensive agri-energy model presented in [16]. The model depicted in Figure 1 was specifically developed to quantify the energy requirements associated with vertical farm operations. The model incorporates the simulation of all major subsystems involved in vertical farm operation, including artificial lighting, humidification and dehumidification, HVACD, and CO<sub>2</sub> enrichment. Environmental control is achieved by modulating key variables to evaluate their impact on both energy demand and crop productivity. Indoor air temperature is maintained at the defined setpoint via heating and cooling systems, while the desired photosynthetic photon flux density (PPFD) is ensured through LED-based lighting. A spray-based humidification system and an Air Handling Unit (AHU) regulate the relative humidity (RH), keeping it within the optimal range for plant growth. CO<sub>2</sub> concentration is controlled through an enrichment system comprising gas cylinders and modulating valves, designed to offset CO<sub>2</sub> uptake by plants and losses through ventilation. To mitigate the accumulation of phytotoxic compounds and ensure air quality, a minimum air exchange rate is provided by the ventilation and filtration system. This comprehensive configuration allows for an accurate assessment of the interactions between environmental control strategies and overall vertical farm performance.

The energy balance within the growing chamber is described in Eq. (1), where each Q-term represents a specific energy flow associated with the subsystems described above. Specifically, Q<sub>Light</sub> denotes the radiant energy supplied by the LED lighting system, while Q<sub>plant</sub> corresponds to the fraction of this energy absorbed and effectively converted by the crop through photosynthesis. The thermal loads Q<sub>h/c</sub> and Q<sub>AHU</sub> are energy loads associated with the Heating/Cooling (HC) system and the AHU, respectively. Q<sub>eva</sub> and Q<sub>hum</sub> represent latent cooling loads associated with the evaporation of water transpired by the crop and introduced by the

humidification system, respectively. Lastly,  $Q_{env}$  accounts for heat exchange with the external environment through the chamber envelope, encompassing both thermal losses and gains.

$$d_{air}c_{p_{air}}V_{room}\frac{\partial T}{\partial t} = Q_{env} + Q_{Light} - Q_{plant} - Q_{eva} + Q_{h/c} - Q_{AHU} - Q_{hum} \quad (1)$$

All these energy flows are extensively detailed in the reference modeling paper [16]. Therefore, only the key equations (2), (3), (4), and (4) are reported in this section to provide the essential energy-related insights. In particular,  $Q_{rad}$  accounts for the net heat transfer through the building envelope due to both incident solar radiation and longwave infrared radiation exchange with the sky.  $Q_{Light}$  includes the total energy emitted by the lighting system, comprising both the luminous component and the associated thermal load. A portion of the luminous energy is absorbed by the crop canopy ( $Q_{abs}$ ), while the remainder is either reflected or converted into thermal energy via evapotranspiration (ET), thereby contributing to the internal thermal load. The fraction of light effectively used for biomass production was estimated by assuming that the change in dry matter (DM) corresponds to glucose synthesis via the photosynthetic reaction.

$$Q_{env} = U_{wall}A_{wall}(T_{in} - T_{ext}) + Q_{rad} \quad (2)$$

$$Q_{rad} = \alpha I + \sigma\varepsilon A(T_{wall}^4 - T_{sky}^4) \quad (3)$$

$$Q_{Light} = \frac{PAR}{F} \cdot A_c \cdot \frac{1}{\eta_{LED}} \quad (4)$$

$$Q_{plant} = \frac{\frac{\partial DM}{\partial t}}{MW} A_c \cdot \Delta E_{photo} \quad (5)$$

The dynamic growth model adopted for lettuce cultivation, previously calibrated and validated, is primarily governed by equations (6) and (7), which describe the instantaneous variation in dry matter (DM) and fresh matter (FM) as functions of key environmental growth factors, namely temperature, CO<sub>2</sub> concentration, and PPFD. At each simulation timestep, the leaf area index (LAI) was computed based on the DM from the previous timestep, a root-to-shoot allocation factor, and the specific leaf area (SLA), which is itself influenced by the prevailing indoor environmental conditions. As the original model was calibrated under a fixed CO<sub>2</sub> concentration of 1200 ppm, an additional correction factor was introduced in this work to account for variations in CO<sub>2</sub> levels. This factor, derived from [19], accounts for the impact of CO<sub>2</sub> concentration on light use efficiency (LUE) as a function of the selected PPFD, thereby enabling a more accurate representation of crop productivity across different atmospheric enrichment scenarios.

$$\frac{dDM}{dt} = PAR \cdot (1 - e^{-k \cdot LAI}) \cdot LUE_{dm} \cdot A_c \cdot f_{CO_2} \quad (6)$$

$$\frac{dFM}{dt} = PAR \cdot (1 - e^{-k \cdot LAI}) \cdot LUE_{fm}(t) \cdot A_c \cdot f_{CO_2} \quad (7)$$

To evaluate the water demand of the VF system, Eq. (8) was applied to estimate the water vapor flux transpired from the leaf surface of lettuce plants. The crop coefficient (K<sub>c</sub>) was experimentally determined in [20] and varies according to the crop's phenological stage. Additional methodological details on this approach are comprehensively discussed in the referenced model study [16]. The total water demand was then quantified by summing the moisture removed by the cooling and AHU systems (m<sub>cond</sub>), the water content retained in the harvested fresh biomass, and the amount of water sprayed by the humidification system

( $m_{hum}$ ), which is especially relevant during the early growth stages to maintain optimal relative humidity, as shown in Equation (9). Finally, the CO<sub>2</sub> uptake by the crop was estimated based on a stoichiometric assumption, whereby the amount of carbon fixed is equivalent to twice the mass of dry biomass produced, following the methodology outlined in [21].

$$\dot{m}_{ET} = 1.05 \cdot \frac{0.408 \cdot \Delta \cdot RAD_n + \frac{900 \cdot u \cdot \gamma \cdot VPD_{in}}{T_{in} + 273.15}}{\Delta + \gamma \cdot (1 + 0.34 \cdot u)} \cdot A_c \cdot K_c \quad (8)$$

$$M_{wat} = \int_{year} (\dot{m}_{ET} + \dot{m}_{hum} - \dot{m}_{cond}) dt + (FM_{tot} - DM_{tot}) \quad (9)$$

All the values for the key parameters presented in these equations are summarized in Table 1.

Table 1: Main assumptions for the VF transient model presented in [16]

Symbol	Value	Unit
$U_{wall}$	0.193	$W m^{-2} K^{-1}$
$F$	3	$\mu mol \cdot J^{-1}$
$\eta_{LED}$	0.85	[–]
$MW$	180	$g mol^{-1}$
$\Delta E_{photo}$	2807	$kJ mol^{-1}$
$u$	0.4	$m s^{-1}$

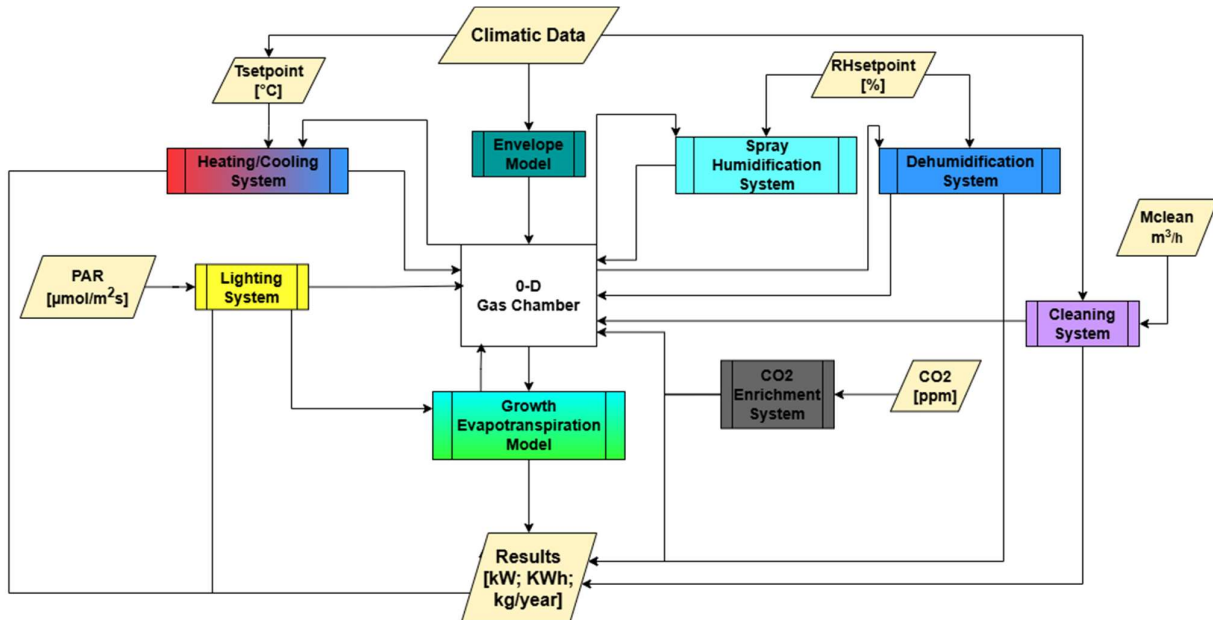


Figure 1: Flowchart of the model developed in Amesim Simcenter

## 2.2. Studied Cases

As outlined in the Introduction, this study aims to evaluate how key environmental parameters influence the resource consumption (energy, water, and carbon dioxide), productivity, and economic feasibility of VF. The primary drivers of crop productivity in VF are indoor air temperature ( $T_{in}$ ), PPF level (PAR), and CO<sub>2</sub> concentration ( $X_{CO2}$ ), which were therefore selected as the core variables under investigation. Indoor temperature not only influences plant growth directly, but also impacts energy losses through the building envelope. Based on the findings of Carotti [6] who identified 24 °C as the most productive temperature

for lettuce, three temperature setpoints ( $20^{\circ}\text{C}$ ,  $24^{\circ}\text{C}$ , and  $28^{\circ}\text{C}$ ) were tested to assess their effect on overall VF performance and consumption metrics. Although varying indoor temperatures inherently alter the vapor pressure deficit (VPD), this study assumes a controlled relative humidity (RH) of 75% during the photoperiod and 85% during the dark period. While RH has not shown a significant direct impact on crop growth rates [17], however, RH does influence the energy consumption of the AHU system. Conversely, PPFD significantly affects the overall energy demand of the VF. Higher PPFD levels directly increase electricity consumption due to the lighting system and indirectly raise the HVACD load, as excess heat generated by the LEDs must be removed to maintain set indoor temperatures. On the other hand, increasing PPFD levels lead to higher crop productivity within the vertical farm. However, this relationship is not linear, as photosynthetic efficiency declines with increasing PPFD. Carotti et al. [6] demonstrated that increasing the PPFD above  $400 \mu\text{mol m}^{-2} \text{s}^{-1}$  is not advantageous, even from an agronomic perspective, as the resulting improvements in crop growth rate are marginal. Based on these findings, the present study explores the effect of three distinct PPFD levels on vertical farm performance: a very low level ( $100 \mu\text{mol m}^{-2} \text{s}^{-1}$ ), a standard reference value ( $250 \mu\text{mol m}^{-2} \text{s}^{-1}$ ), and a high level ( $400 \mu\text{mol m}^{-2} \text{s}^{-1}$ ), in order to assess their impact on both productivity and energy consumption. Although the positive effect of CO<sub>2</sub> enrichment on crop growth has been well established, and CO<sub>2</sub> concentration does not directly influence the energy consumption of the vertical farm, it is still relevant to quantify its impact on productivity. This allows for a meaningful comparison between the yield gains and the associated increase in operational expenditures due to carbon fertilization. For this reason, three levels of CO<sub>2</sub> concentration were tested in this study: ambient (400 ppm), moderate enrichment (900 ppm), and high enrichment (1400 ppm).

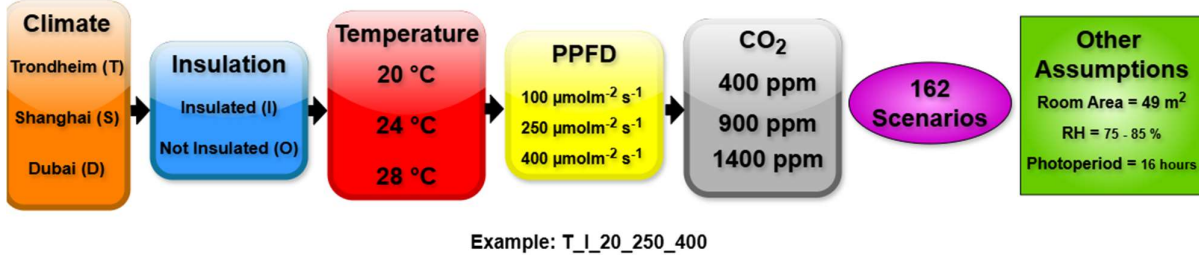
From an energy perspective, as highlighted in the current literature, vertical farming systems typically require substantial cooling loads to dissipate the thermal energy generated by LED lighting. Consequently, assessing the influence of the thermal insulation layer on the VF's energy consumption becomes noteworthy. In this study, two building envelope configurations were simulated: one equipped with a 105 mm thick rigid polyurethane (PUR) insulation layer, and one without any insulation. The impact of insulation on overall energy consumption is intrinsically linked to the external climatic conditions. To account for this, three distinct climate scenarios were selected, each representative of different latitudes and weather profiles, as well as varied socio-economic contexts. Specifically, the cities of Trondheim (cold climate), Shanghai (temperate climate), and Dubai (hot climate) were chosen. These metropolitan areas were selected not only for their contrasting climates but also because urban settings are particularly relevant for vertical farming due to land use constraints and urban food production potential. Hourly data for ambient temperature, relative humidity, and solar irradiation were obtained from [33] for the three locations. Additionally, the geographic coordinates of each city were used to compute altitude and azimuth angles, allowing for an accurate estimation of solar gains on the vertical farm's external surfaces.

All scenarios described above were simulated using the model presented in [16], assuming a square growing chamber with 7-meter sides and a height of 3 meters. The chamber was equipped with five three-tier shelving units, resulting in a net cultivated area of  $90 \text{ m}^2$  (61% land use efficiency per single tier). Lettuce crops were cultivated at a density of 25 plants per

square meter, under a 16-hour photoperiod, and harvested upon reaching an average fresh weight of 250 g per plant [6].

All the analyzed scenarios are summarized in Figure 2, and from this point onward, they will be referenced using the acronyms reported therein. To evaluate the influence of each variable on the energy requirements, crop productivity, and water use efficiency (WUE) of the vertical farm, previous studies such as [14] employed the Spearman rank correlation coefficient. However, due to the non-linear relationships among the variables analyzed in this study, the distance correlation coefficient has been used instead. This metric was calculated according to Eq. 10, where  $dCov(X,Y)$  represents the distance covariance between two variables (X, Y), and  $dVar$  refers to their distance variance. Further details regarding the calculation procedure are provided in the Appendix. A distance correlation coefficient ( $\rho$ ) approaching 1 indicates a strong correlation between the variable and the outcome, while a value of  $\rho$  near 0 suggests a negligible or no correlation.

$$\rho(X, Y) = \frac{dCov(X, Y)}{\sqrt{dVar(X) \cdot dVar(Y)}} \quad (10)$$



Example: T\_I\_20\_250\_400

Figure 2: Input conditions for the scenarios assessed by sensitivity analysis.

### 2.3. Economic and Sustainability Analysis

The feasibility of a VF is significantly influenced by its location. Therefore, this section outlines all assumptions related to the costs and emissions associated with lettuce production in vertical farming systems. In line with the objective of decarbonizing the agricultural sector through electrification [18], two air-to-water heat pumps (HPs) were employed to be employed to meet the energy demands for heating, cooling, and dehumidification within the HVACD system. The electricity consumption of the HPs was defined in Eq. (11). The coefficient of performance (COP) was calculated using an algorithm that considers for the nominal COP ( $COP_{nom}$ ) (which depends on the HP size), external temperature, indoor temperature and part-load factor (PLF) as described in Eq. (12). For the HP used for heating purpose, the dependencies of the COP on temperature ( $COP_T$ ) and part-load factor were sourced from [22] and [23]. For the unit used for cooling and dehumidification, data were obtained from [24]. This method is deemed more accurate than the exergy efficiency assumptions reported in [16]. The nominal COP values for the HPs were determined based on commercial data provided in the AERMEC catalogue[25], considering the appropriate duty. Further methodological details can be found in [16].

$$P_{HP}(t) = \frac{Q_{HP}(t)}{COP(t)} + 0.008 \cdot Q_{HP}(t) \quad (11)$$

$$COP(t) = COP_{nom} \cdot \frac{COP_T(T_{ext}, T_{wat})}{COP_T(T_{ext,nom}, T_{wat})} \cdot PLF(PLR) \quad (12)$$

The first step in evaluating the feasibility of the VF involved assessing the capital expenditures (CAPEX) required for its implementation. Assuming the building structure is already in place, the fixed expenditures include the lighting system, electrical wiring, HVACD system, growing chamber, and insulation layer installation. These assumptions were reported in Table 2. These costs were considered location-independent, and a linear scaling function was applied to estimate the total investment. The specific costs for lighting, wiring, growing, and HVACD, sourced from [26], were adjusted (+27%) using the Consumer Price Index (CPI) trend from 2018 to 2025, as reported by the U.S. Bureau of Labor Statistics[27]. The LED cost per W reported in [26] was based on an LED efficiency of  $1.48 \mu\text{mol m}^{-2} \text{s}^{-1}$ ; therefore, this value was doubled to reflect the higher LED efficiency adopted in this study. Additionally, the purchasing cost of the polyurethane rigid foam (PUR) used for insulation was increased by 40% to account for installation expenses [28].

Table 2: Assumed costs for vertical farm purchase [26], [28].

<b>Symbol</b>	<b>Value</b>	<b>Attualized Value</b>	<b>Unit</b>
$c_{Light}$	1.48	3.76	$\$ \text{W}^{-1}$
$c_{Wir}$	0.85	1.08	$\$ \text{W}^{-1}$
$c_{HVACD}$	1.092	1.39	$\$ \text{W}^{-1}$
$c_{VF}$	224	284.5	$\$ \text{m}_{crop}^{-2}$
$c_{Ins}$	20	28	$\$ \text{m}^{-2}$

Since all scenarios were analyzed and compared over a year-long simulation, it is essential to estimate the annual operational expenditures (OPEX) associated with the lettuce production. Table 3 summarizes the reference prices adopted in this section. The OPEX includes crop-related costs (seeds, nutrients, and packaging), expressed in \$ per kilogram of lettuce produced, as well as costs for electricity, water, carbon dioxide, labor, and land leasing. Crop-related costs were assumed to be location-independent. Conversely, electricity, water, labor, and leasing prices were evaluated based on the specific conditions of each study location. In recent years, the price of carbon dioxide has risen, partly due to increased demand for carbon fertilization [29]. Therefore, an average global price of  $3.5 \$ \text{kg}^{-1}$  was adopted. Labor costs were estimated under the assumption that workers are trained agronomists, with a labor requirement of 0.067 hours per kilogram of lettuce produced [30]. Lastly, land leasing costs were assessed based on average rental prices of warehouses in the selected cities.

Table 3: Assumed costs for estimating operational expenditures.

<b>Symbol</b>	<b>Trondheim</b>	<b>Shanghai</b>	<b>Dubai</b>	<b>Unit</b>
$c_{crop}$	1.14 [26]	1.14 [26]	1.14 [26]	$\$ \text{kg}^{-1}$
$c_{CO2}$	3.50 [31][32]	3.50 [31][32]	3.50 [31][32]	$\$ \text{kg}^{-1}$
$c_{el}$	0.10[33]	0.09[34]	0.11[35]	$\$ \text{kWh}^{-1}$
$c_{wat}$	2.90[36]	0.48[34]	2.51[35]	$\$ \text{m}^{-3}$
$c_{Lab}^1$	33.33[37]	14.43[37]	30.93[37]	$\$ \text{h}^{-1}$
$c_{Leas}$	143.40 [38]	50.10[39]	168.50 [40]	$\$ \text{m}^{-2}$

<sup>1</sup> The referenced source provides the comprehensive dataset used to determine the average hourly wage for each location.

The aforementioned assumptions have been applied to evaluate both the capital expenditure (CAPEX) and the operational expenditure (OPEX) of the studied vertical farms using Equations 13 and 14. Since the key parameter for the economic assessment is the levelized cost of lettuce (LCoL), an average system lifetime ( $n$ ) of 20 years [41] and a nominal interest rate ( $r_{nom}$ ) of 8.5 percent, as typically assumed for agricultural investments [42] have been considered. Assuming an inflation rate of 2%, the real interest rate ( $r_{real}$ ) has been calculated (see Eq. 15). This rate has been used to determine the capital recovery factor (CRF), which is then applied to annualize both the initial investment (CAPEX) and the replacement costs. Given that the estimated lifespan of the LEDs is shorter than the overall system lifetime of 20 years, the cost of replacing the lighting system ( $C_{Rep}$ ) has been included twice: once after 8 years and once again after 16 years from the start of operations. These future expenses have been converted to their present value using the real interest rate, as described in Equation 16. Finally, the sum of the annualized investment and replacement costs, along with the annual OPEX, has been divided by the annual crop yield of the VF to calculate the LCoL, as outlined in Equation 18.

$$CAPEX = c_{Light} \cdot P_{Light} + c_{Wir} \cdot (P_{Light} + P_{HVACD}) + c_{HVACD} \cdot P_{HVACD} + c_{VF} \cdot A_c + c_{Ins} \cdot A_{env} \quad (13)$$

$$OPEX = M_{crop} \cdot c_{crop} + E_{el} \cdot c_{el} + M_{wat} \cdot c_{wat} + M_{CO2} \cdot c_{CO2} + h_{lab} \cdot c_{lab} + A_{VF} \cdot c_{leas} \quad (14)$$

$$r_{real} = \frac{(1-r_{nom})}{(1-i)} - 1 \quad (15)$$

$$CRF = \frac{r_{real} \cdot (1+r_{real})^n}{(1+r_{real})^n - 1} \quad (16)$$

$$C_{Rep} = (c_{Light} \cdot P_{Light}) \cdot \left( \frac{1}{(1+r_{real})^8} + \frac{1}{(1+r_{real})^{16}} \right) \quad (17)$$

$$LCoL = \frac{(CAPEX + C_{Rep}) \cdot CRF + OPEX}{M_{crop}} \quad (18)$$

Ultimately, the energy mix of the selected locations, as reported in [43], [44], [45] was used to estimate the carbon emissions associated with vertically grown lettuce. To provide a benchmark for lettuce-related carbon emissions, transport-related emissions from imported lettuce were also calculated for each location, based on the assumptions listed in Table 4. The supply chain for each location and the corresponding mode of transport (refrigerated truck, refrigerated ship, or airplane), chosen according to the supply distance. The exporting country for each location was identified using data provided by the World Integrated Trade Solution [46], [47], [48]. In this study, truck transportation is assumed to be carried out using a 32-ton articulated vehicle, with an average payload of 9.33 t (corresponding to 90% of the total capacity) and an average volume load of 14.38 pallets. To estimate specific carbon emissions, chilled single-drop distribution is considered, along with an average annual refrigerant leakage of 15% R404A [49]. Assuming a lettuce density of 200 kg m<sup>-3</sup> and an available refrigerated container volume of 27 m<sup>3</sup> (90% of 1 twenty-foot equivalent unit (TEU)), emission data corresponding to average speed and refrigerated containers, as reported in [50], were used. Airplane-related emissions are assumed to range from 4 to 10 times higher than those of maritime transport [51], therefore, an average multiplier of 7 was applied to estimate emissions from air freight.

Table 4: Assumption for estimating the difference in CO<sub>2</sub> emissions difference between local and imported lettuce.

<b>Symbol</b>	<b>Trondheim</b>	<b>Shanghai</b>	<b>Dubai</b>	<b>Unit</b>
Export Country	Spain	Korea	Spain	–
$L_{supply}$	3400	1000	5000	km
Transport	Truck (100%)	Truck (20%) + Ship (80%)	Truck (5%) + Airplane (95%)	–
$e_{VF}$	15	585	404	ton <sub>CO<sub>2</sub></sub> /GWh
$e_{truck}$	98.30	98.30	98.30	g <sub>CO<sub>2</sub></sub> /(ton · km)
$e_{ship}$	35.71	35.71	35.71	g <sub>CO<sub>2</sub></sub> /(ton · km)
$e_{airplane}$	250.00	250.00	250.00	g <sub>CO<sub>2</sub></sub> /(ton · km)

### 3. Results

#### 3.1. Crop Growth Results

As highlighted in related studies, indoor temperature, PPF, and CO<sub>2</sub> concentration significantly influence the lettuce growth rate in VF systems. Figure 3 illustrates the contribution of each parameter to the duration of the growth cycle, defined as the number of days from transplanting to harvest. The figure clearly shows that the effect of carbon fertilization diminishes as PPF increases. Specifically, at a PPF of 100 μmol m<sup>-2</sup> s<sup>-1</sup>, elevated CO<sub>2</sub> concentration resulted in a growth cycle 31% shorter than under ambient conditions (400 ppm). However, at a PPF of 400 μmol m<sup>-2</sup> s<sup>-1</sup>, the reduction in growth duration decreased to 22%. Notably, increasing CO<sub>2</sub> concentrations beyond 900 ppm had a limited effect on lettuce growth, and in some cases, even led to a slight decline in performance under the highest PPF conditions.

The effect of PPF is more pronounced at lower indoor temperatures, and its influence on the growth rate is not linear with light intensity, as the LUE is also affected by PPF levels. In particular, above 250 μmol m<sup>-2</sup> s<sup>-1</sup>, LUE decreases significantly, resulting in the asymptotic trend observed in the figure. This trend shows that, for each combination of indoor temperature and CO<sub>2</sub> concentration, the reduction in the crop growth cycle due to increasing PPF becomes progressively smaller as PPF continues to rise.

The impact of temperature on crop growth is relatively limited. Increasing the indoor temperature to 24°C and 28°C resulted in a reduction of the growth cycle by 17% and 14%, respectively. However, higher temperatures slightly reduce LUE, which in turn diminishes the positive effect of increased PPF on crop growth. For example, at 20°C, increasing the PPF to 400 μmol m<sup>-2</sup> s<sup>-1</sup> results in a 20.5% reduction in the growth cycle. Under the same PPF increase, the corresponding reductions at 24°C and 28°C decrease to 18.4% and 7%, respectively. Overall, crop productivity ranged from 31 to 118 kg m<sup>-2</sup> per year, which is equivalent to the output of an open field area of approximately 550 to 2100 m<sup>2</sup>. Consequently, vertical farming demonstrated a land use efficiency between 11 and 43 times higher than that of conventional open-field farming.

In conclusion, for the crop production perspective, the optimal indoor conditions within the growing chamber are an indoor temperature of 24°C, a PPF level of 400 μmol m<sup>-2</sup> s<sup>-1</sup>, and a CO<sub>2</sub> concentration of 900 ppm, resulting in a crop growth cycle of only 19 days. This

result is consistent with the findings reported in [6], where the highest productivity was achieved at the highest PPF. While PPF levels above  $400 \mu\text{mol m}^{-2} \text{s}^{-1}$  might further reduce the growth cycle duration, such scenarios were not considered in this study, as previous research has shown that the additional energy demand would outweigh the production benefits.

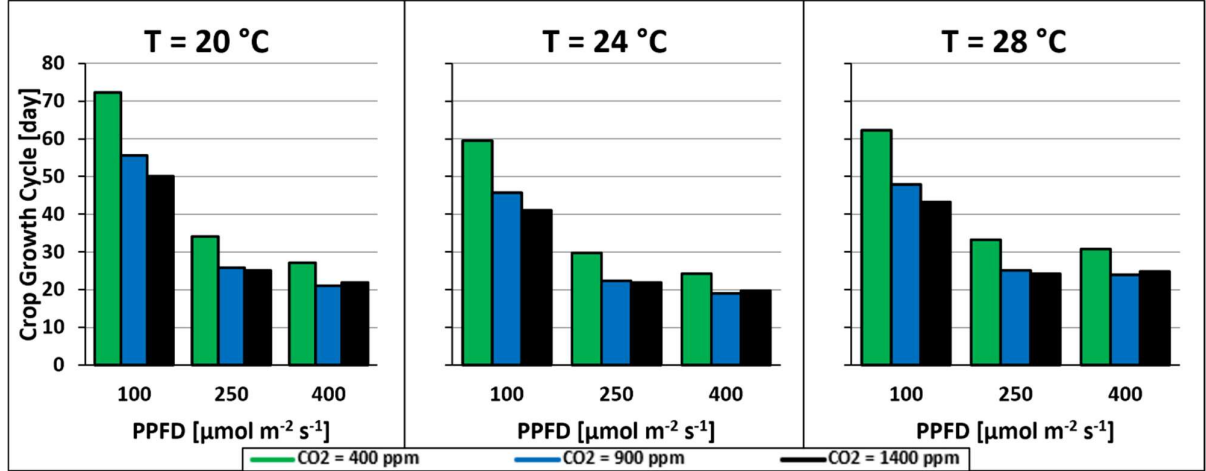


Figure 3: Effect of indoor condition (Temperature, PPF, and  $\text{CO}_2$  concentration) on crop growth cycle length.

### 3.2. Vertical Farm Thermal Demand

The thermal demand of a vertical farm (VF) comprises the heating required to maintain suitable temperatures in the growing chamber, particularly during dark periods, the cooling necessary to remove excess heat generated by the lighting system, and the dehumidification combined with post-heating (PH) needed to eliminate surplus moisture transpired by the plants. All these energy fluxes are influenced by indoor conditions, such as temperature and PPF, as well as by the external climate.  $\text{CO}_2$  concentration also affects the VF's energy demand, primarily through its impact on crop growth. Consequently, since both cooling and dehumidification loads are closely linked to plant growth, they are indirectly influenced by  $\text{CO}_2$  concentration. However, given that this effect is relatively minor, with annual energy demand variations due to  $\text{CO}_2$  levels remaining below 2%, this parameter will not be explicitly represented in the energy demand analysis.

Among the aforementioned thermal energy fluxes, the cooling load is the most significant, as illustrated in Figure 4, which shows the energy fluxes in an insulated VF, under conditions of  $20^\circ\text{C}$  and  $100 \mu\text{mol m}^{-2} \text{s}^{-1}$ , based on year-round simulations in the three selected locations. The cooling system also contributes to indoor moisture control by condensing and removing part of the air's water content. As a result, higher cooling loads are typically associated with lower dehumidification requirements. As previously discussed, both cooling and dehumidification loads are influenced by the crop growth stage. During early growth stages, evapotranspiration is limited due to the small leaf surface area, and spray humidification is often required to maintain the desired relative humidity by compensating for the moisture removed through cooling. This humidification flux provides a "free cooling" effect, thereby reducing the net cooling load. Conversely, during later growth

stages, evapotranspiration increases significantly, which raises the dehumidification demand. At the same time, spray humidification is no longer needed, eliminating the free cooling effect and increasing the cooling load again. These dynamics result in a characteristic wavy trend of the cooling load over time. These trends are clearly observable in Figure 4 and in Figures A1–A8 presented in the Appendix.

Figures A1–A8 present the thermal load trends for all simulated scenarios and are included in the Appendix to improve the manuscript's readability and reduce its length. Despite being placed in the supplementary section, these figures clearly illustrate the effects of the three investigated parameters (indoor temperature, PPFD, and geographic location) on the required thermal loads.

As previously discussed, PPFD is closely linked to both cooling and dehumidification loads. As light intensity increases, the amount of heat that must be removed from the growing chamber also rises. However, the increase in cooling demand is not linear with PPFD, as the proportion of light absorbed and converted by the crop (LUE) varies with light intensity. Specifically, increasing the PPFD from 100 to 250 and 400  $\mu\text{mol}\cdot\text{m}^{-2}\cdot\text{s}^{-1}$  results in a 180% and 360% increase in cooling load, respectively. Conversely, the dehumidification load decreases significantly (by 67% and 77%, respectively), since the cooling system itself removes substantial amounts of moisture from the air. This occurs because, when the PPFD exceeds 100  $\mu\text{mol m}^{-2} \text{ s}^{-1}$ , the dehumidification system operates primarily during dark periods, when lighting and, consequently, cooling, are inactive. Finally, as the heating demand in a vertical farm arises predominantly during dark periods and is largely independent of the lighting intensity, PPFD does not affect the heating load.

Thanks to the insulation layer, the effect of indoor temperature on cooling demand remains relatively limited. Specifically, increasing the indoor temperature from 20 °C to 28 °C results in a reduction of cooling load by approximately 8.5% to 10%, depending on the external climate. However, despite the insulation, the influence of external climate conditions on the heating load remains significant. In particular, increasing the indoor temperature from 20 °C to 28 °C leads to a 50% increase in heating demand in a cold climate (e.g., Trondheim) and up to 360% in a hot climate (e.g., Dubai). Moreover, since indoor temperature affects relative humidity by increasing the allowable vapor pressure deficit (VPD) by approximately 60%, the dehumidification load decreases by 48% and 58% in cold and hot climates, respectively, when the indoor temperature is raised from 20 °C to 28 °C.

Consequently, the impact of geographic location on an insulated vertical farm is relatively limited, as illustrated in Figure 4. However, humid climates can slightly increase the dehumidification load due to the higher moisture content of the outdoor air used by the air exchange system, which is necessary to remove potentially harmful compounds produced during photosynthetic reactions. In conclusion, among all the tested scenarios, the configuration identified as T\_I\_100\_28\_900, characterized by a cold climate, low PPFD, and high indoor temperature, resulted in the lowest overall thermal energy demand, with an annual thermal load of 18 MWh<sub>th</sub>.

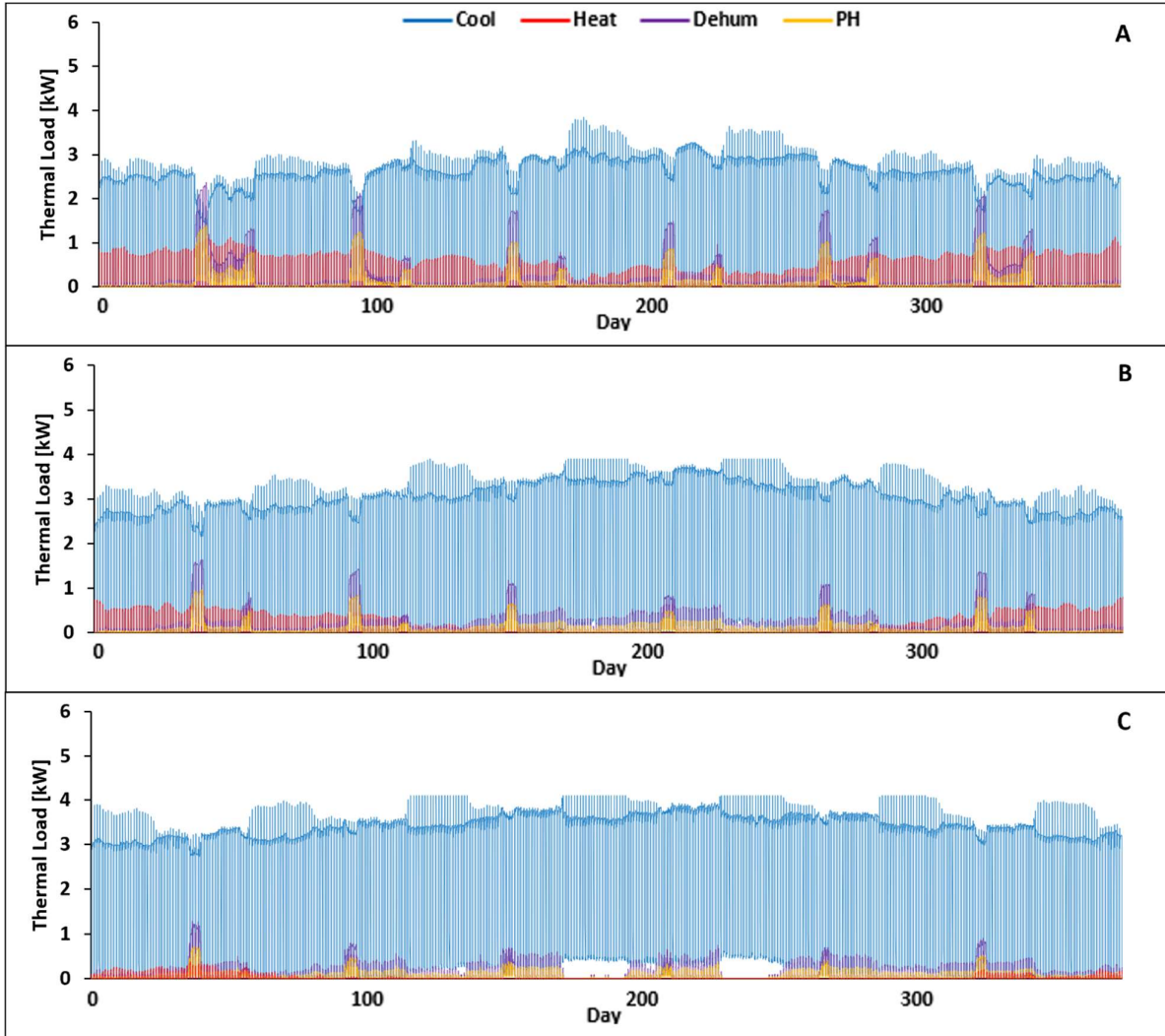


Figure 4: Heating, cooling, dehumidification and post-heating loads throughout the year for a well-insulated VF in three locations: (A) Trondheim, (B) Shanghai, (C) Dubai. The results were obtained under conditions of 20 °C and 100  $\mu\text{mol m}^{-2} \text{s}^{-1}$ .

The following paragraphs aim to highlight the impact of the insulating layer on the various heat fluxes across the studied locations. While in the insulated VF the heating and cooling loads are relatively independent of the external climate, Figure 5, based on the same sample scenario shown in Figure 4, illustrates how these loads are significantly influenced by outdoor conditions in the absence of insulation. The thermal loads for all other scenarios are comprehensively represented in Figures A9–A16, included in the Appendix. As shown, without an insulating layer, the cooling and heating loads exhibit opposite trends. Specifically, in cold climates and under low PPFD conditions, the heating system operates even during light periods when the LEDs are on. Conversely, in hot climates, the cooling system remains active even during dark periods to counteract heat gains through the building envelope. The dehumidification load tends to increase in scenarios where cooling demand decreases, primarily due to heat losses through the envelope, which is a typical characteristic of cold climates.

In cold climates, when both PPFD and indoor temperature are low, the heating load can increase by 360% compared to the insulated scenario, while the cooling demand is reduced by approximately 70%. However, this reduction in cooling load leads to an increase in both

dehumidification and post-heating loads, resulting in an overall thermal energy increase of about 40%. This deterioration in energy performance becomes more pronounced as the indoor temperature rises, since heat losses through the building envelope are directly proportional to the temperature gradient between indoor and outdoor environments. At an indoor temperature of 28 °C and the same PPFD, the total energy consumption increases by 75% compared to the corresponding insulated case. As higher PPFD levels elevate the cooling demand, the negative effect of removing the insulating layer is partially mitigated. For instance, at a PPFD of 400  $\mu\text{mol m}^{-2} \text{s}^{-1}$  and an indoor temperature of 20 °C, the heating load increases by 280%, while the cooling and dehumidification loads decrease by around 11%. Overall, this results in a slight reduction in total energy consumption of about 4%, which can increase to 5% at higher indoor temperatures.

Conversely, under hot climates conditions, the absence of an insulating layer has a limited impact on the heating load, given that the majority of the thermal gains is due to the lighting system. When the indoor temperature is maintained at 20°C, the heating load increases by approximately 107% In contrast, the cooling load rises by 7–27%, depending on the PPFD level. The higher the PPFD, the smaller the relative impact of the insulating layer on total energy consumption. Notably, at low PPFD values, the overall increase in thermal energy consumption ranges between 6% and 21%, depending on the indoor temperature, figures that are considerably lower than those observed in corresponding cold-climate scenarios. Nevertheless, in all studied cases, the removal of the insulating layer in VFs located in hot climates results in an increase in total thermal energy demand. Among the tested scenarios, the one most resilient to the absence of insulation is characterized by an indoor temperature of 28 °C and a PPFD of 400  $\mu\text{mol m}^{-2} \text{s}^{-1}$ .

In conclusion, the lowest total energy consumption among the non-insulated VF scenarios was observed in configuration D\_O\_100\_28\_900, with an annual thermal energy demand of 21 MWh<sub>th</sub>. However, the removal of the insulating layer can only be considered

a viable strategy under specific conditions, namely, in colder climates where both the indoor temperature and PPFD are maintained at high levels.

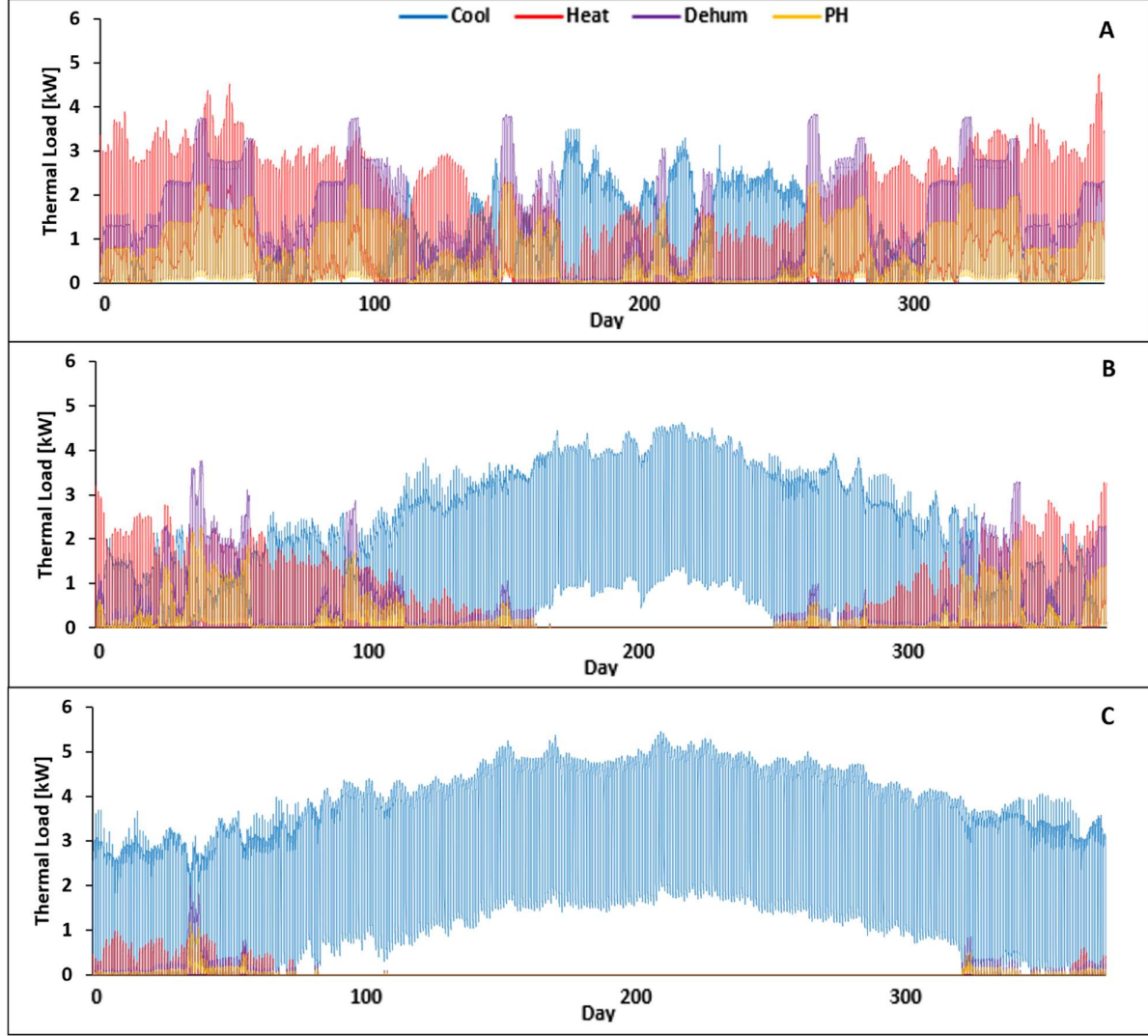


Figure 5: Heating, cooling, dehumidification and post-heating loads throughout the year for a not-insulated VF in three locations: (A) Trondheim, (B) Shanghai, (C) Dubai. The results were obtained under conditions of 20 °C and 100  $\mu\text{mol m}^{-2} \text{s}^{-1}$ .

### 3.3. Specific Energy Consumption and Water Use Efficiency

As highlighted in the previous section, the insulating layer plays a modest role in the VF's energy performance. Although the absence of insulation may reduce energy consumption under conditions of high indoor temperature and high PPFD, i.e., when the crop's LUE is lower, insulating the VF remains preferable from an energy efficiency standpoint in hot climates, or under low to medium PPFD levels. Therefore, only the specific energy consumption (SEC) of the simulated insulated scenarios is presented in Figure 6, while the corresponding SEC values for non-insulated scenarios are provided separately in Figure A17 in the Appendix.

In all simulated scenarios where the VF is properly insulated, it is evident that the specific energy demand (SEC) is primarily driven by the PPFD. In fact, LED lighting

and the associated cooling load required to dissipate the heat generated by the lighting system account for over 95% of the total SEC, regardless of the indoor temperature or geographic location. Overall, the SEC ranges from 7.8 to 23.8 kWh kg<sup>-1</sup>, with the lowest values observed in scenarios combining low PPFD, high CO<sub>2</sub> concentration, and an indoor temperature of 24 °C. Increasing the indoor temperature from 20 °C to 24 °C results in an SEC reduction of 11–24%, depending on the PPFD level, with the greatest savings occurring at the lowest PPFD. At 28 °C, further energy savings are marginal for low PPFD scenarios, while at 400 μmol m<sup>-2</sup> s<sup>-1</sup>, raising the temperature to 28 °C leads to a 13% increase in SEC. For PPFD levels of 100 or 250 μmol m<sup>-2</sup> s<sup>-1</sup>, higher CO<sub>2</sub> concentrations correlate with lower SEC, due to the enhanced crop growth rates. However, at higher PPFD levels, the optimal CO<sub>2</sub> concentration appears to be 900 ppm, beyond which the benefits plateau or diminish. Ultimately, scenarios with lower PPFD result in the lowest SEC. According to the experimental data reported by Carotti et al., this outcome is attributable to the increase in light use efficiency (LUE) and specific leaf area (SLA) as PPFD decreases. Both factors contribute to faster crop growth, thereby enhancing productivity relative to the amount of incoming light energy. However, this improvement in energy efficiency comes at the cost of reduced crop productivity per unit area, which drops from 118 kg m<sup>-2</sup> (at 400 μmol m<sup>-2</sup> s<sup>-1</sup>) to 55 kg m<sup>-2</sup> (at 100 μmol m<sup>-2</sup> s<sup>-1</sup>). Nevertheless, from a strictly energy consumption standpoint, the most favorable configuration is T\_I\_100\_24\_1400.

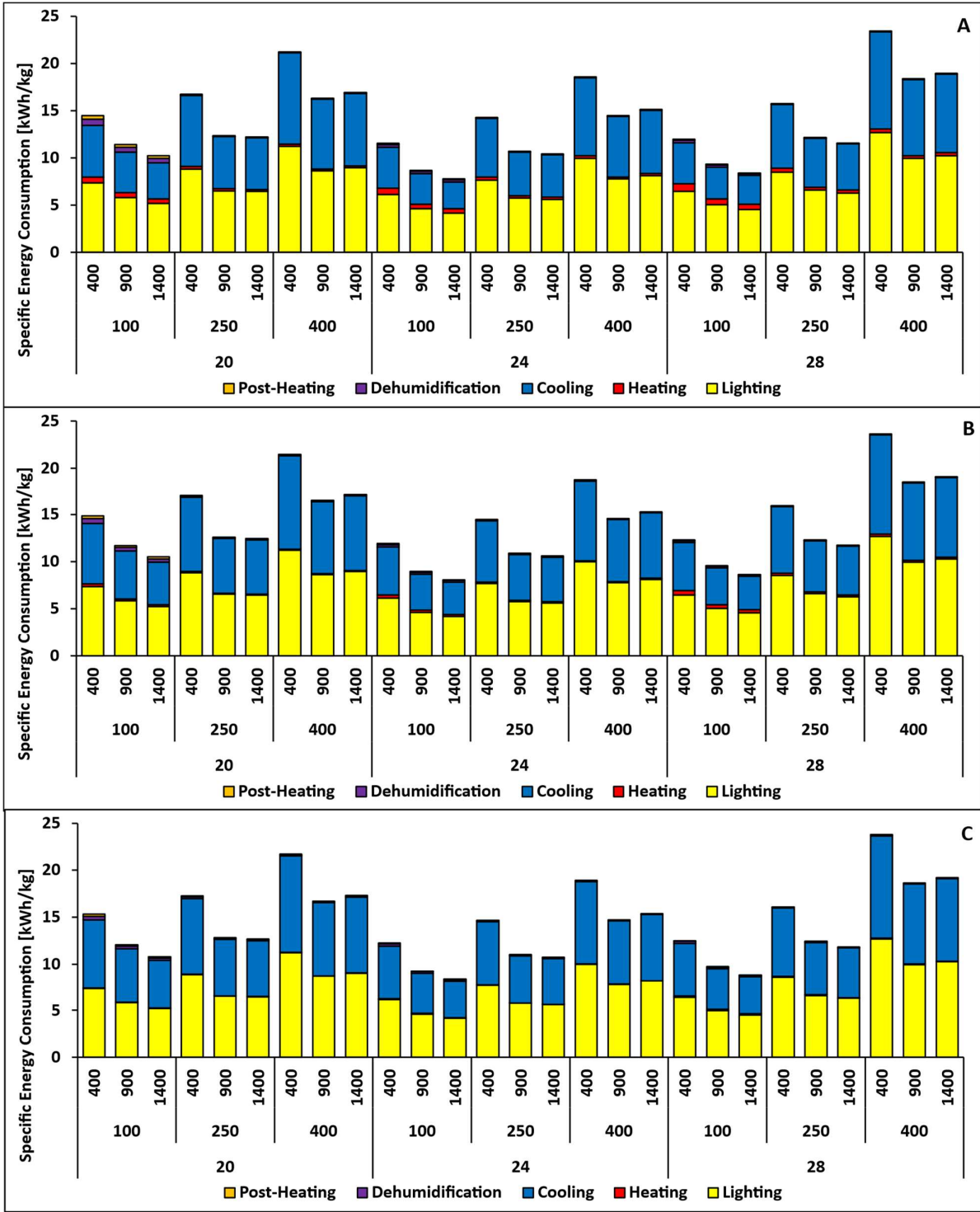


Figure 6: Specific Energy Consumption of the VF under the three simulated locations: (A) Trondheim, (B) Shanghai, (C) Dubai.

The water consumption of vertical farming systems represents a critical indicator of their overall performance. One of the most significant advantages of VF compared to open-field and greenhouse cultivation lies in the potential to recover nearly 100% of the water used. Water use efficiency (WUE) is defined as the ratio between the total fresh weight of lettuce produced and the net water consumption of the system. The net water

requirement is calculated as the difference between the total amount of water supplied, which includes both the water absorbed by the crops and the water added through the humidification system, and the water recovered during the cooling and dehumidification processes. Figure 7 presents the contributions of each water input and the corresponding water use efficiency values for all the simulated scenarios in the Trondheim location. Since the differences in water requirements between different climates remain below 2%, only the Trondheim values for this parameter have been reported to improve the readability of the paper. However, the water use efficiency values for all locations are illustrated in the same figure. Specifically, the water absorbed by the crops consists of the sum of the evapotranspiration flux (ET) and the water content retained within the harvested lettuce (Crop).

The indoor temperature influences WUE by slightly reducing its value as the temperature increases. This effect is explained by the fact that the increase in crop growth associated with higher indoor temperatures is not sufficient to offset the additional water required by the system. In particular, the humidification flow (Hum) is the most affected component, showing increases of 68% and 82% when the indoor temperature rises from 20°C to 24°C and from 24°C to 28°C, respectively.

Light intensity also affects WUE by increasing all of the vertical farm's water streams. Once again, the humidification system is the most impacted by this parameter, as the amount of water required to compensate for humidity condensed and removed by the cooling system is directly proportional to light intensity. Specifically, higher photosynthetic photon flux density (PPFD) levels lead to greater cooling demands, which in turn result in higher amounts of water being removed from the system. In cold climates, increasing the PPFD from 100 to 400  $\mu\text{mol m}^{-2} \text{s}^{-1}$  results in a WUE improvement ranging from 6% to 15%, depending on the indoor temperature. Conversely, in hotter climates, this increase is slightly less pronounced. Furthermore, at an indoor temperature of 20°C, the trend is reversed, with WUE decreasing as the PPFD increases.

The effect of carbon dioxide concentration on WUE is relatively limited. Higher CO<sub>2</sub> levels accelerate crop growth, resulting in only minor changes in WUE. These variations are primarily influenced by external temperature and relative humidity, which affect both heat losses through the building envelope and the moisture content of the air used for cleaning purposes.

Ultimately, the impact of external climate remains significant, even when the vertical farm is well-insulated. While different climates do not substantially affect the total water demand of the VF, higher moisture content in the incoming cleaning air leads to an increase in the amount of water condensed and removed by the chiller and the AHU. As a result, the volume of recovered water increases considerably, allowing the WUE to exceed its theoretical maximum (defined as 1000 plus the dry matter content, DMC). Consequently, a VF located in a hot and arid climate benefits from a notable reduction in net water requirement, with this reduction becoming more pronounced as the indoor temperature decreases. Generally, this translates into lower water consumption and improved WUE, although some of the recovered water is inevitably

lost during indoor air exchanges. In extremely hot climates, at lower indoor temperatures, approximately 240 kg of water per year can be extracted from the external air, reducing the VF's annual water requirement by around 10% in the most favorable scenario. Therefore, from a water use efficiency perspective, the configuration identified as D\_I\_100\_20\_400 proved to be the most optimal, achieving a WUE of 1132 g L<sup>-1</sup>.

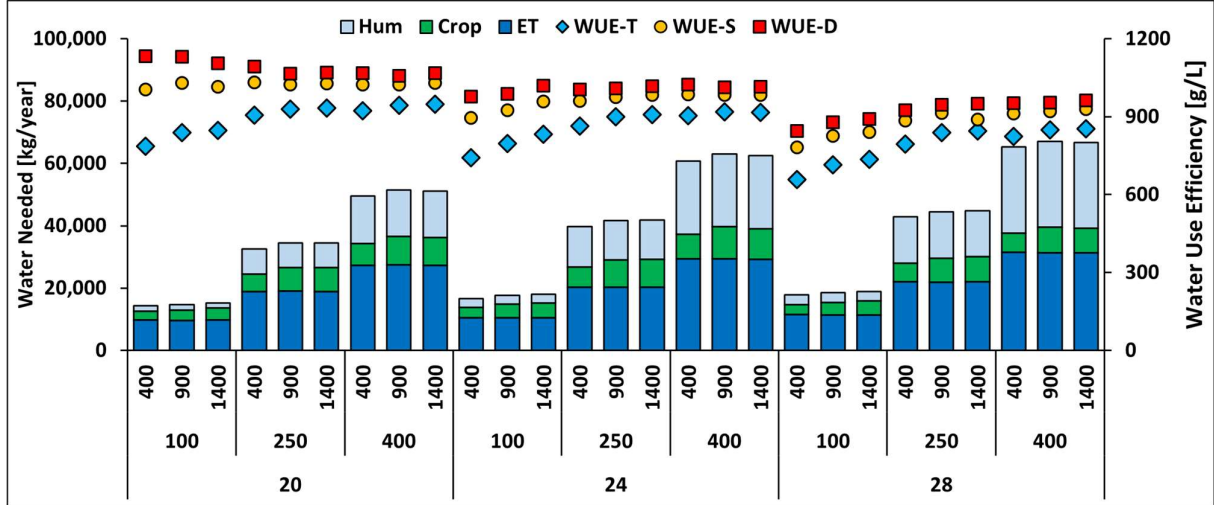


Figure 7: Annual Water requirement and Water Use Efficiency achieved by VF under different indoor conditions in the three locations: (A) Trondheim, (B) Shanghai, (C) Dubai.

### 3.4. Distance Correlation Coefficient Analysis

This section aims to provide a formal assessment of how each input variable influences the main outcomes and performance indicators of the vertical farm. Figure 8 presents the distance correlation coefficients ( $\rho$ ) between the considered input parameters, namely indoor temperature, PPF level, CO<sub>2</sub> concentration, envelope insulation, and external climate, and the key performance indicators, including crop production, water use efficiency, and specific energy demand.

The indoor temperature has a limited influence on crop production, with a distance correlation coefficient of 0.18, primarily due to its effect on the crop's light use efficiency. Similarly, its impact on the specific energy Consumption remains relatively modest, with a coefficient of 0.22, largely attributable to the non-insulated scenarios. Conversely, indoor temperature shows a stronger correlation with water use efficiency, reaching a coefficient of 0.59, as it significantly affects the allowable VPD associated with the relative humidity setpoint.

As previously mentioned, the PPF level is the primary factor influencing both crop production, with a distance correlation coefficient of 0.85, and SED, with a coefficient of 0.73. In comparison, its impact on water use efficiency is more limited, with a coefficient of 0.34. Notably, when considering only the total energy demand, the correlation coefficient for PPF reaches 0.99 clearly indicating that this is the most significant parameter affecting the energy footprint of the vertical farm.

The CO<sub>2</sub> concentration influences all the reported outcomes due to its effect on crop production. Its impact on crop production is more significant than that of indoor temperature, with a distance correlation coefficient of 0.36. Although CO<sub>2</sub> concentration

does not directly affect the vertical farm's energy consumption, it does influence the specific energy consumption through its effect on crop productivity, as reflected by a coefficient of 0.44.

Ultimately, climate and insulation do not affect crop production, as the VF's HVACD system is capable of maintaining the desired indoor conditions regardless of external factors. Since lighting consumption is the primary driver of the specific energy demand, the effect of the insulation layer on this outcome remains relatively small, with a correlation coefficient of 0.08. By influencing the cooling load, the insulation layer also has a minor indirect effect on the water use efficiency, represented by a coefficient of 0.07. Conversely, the external location significantly impacts the VF's water use efficiency, due to the varying moisture content of the air used for cleaning purposes, resulting in a correlation coefficient of 0.62.

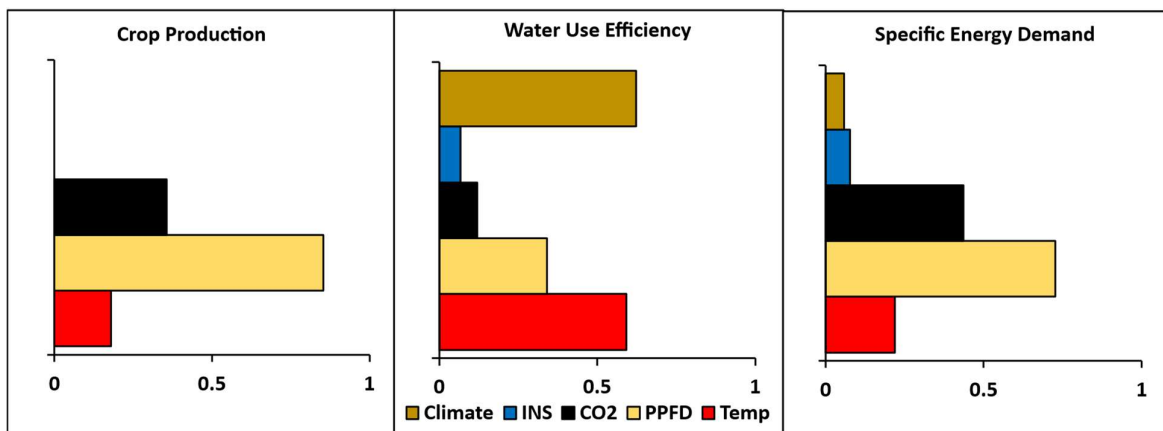


Figure 8: Distance correlation coefficient of input parameters on resource consumption in vertical farming.

### 3.5. VF Electricity Consumption

Economic assessment of the simulated vertical farms requires converting thermal energy demand into electrical power load, which was performed by modelling two air-to-water heat pumps, as described in the methodology section. One heat pump is dedicated to meeting the heating and post-heating demands, while the other is responsible for the cooling and dehumidification requirements. Due to the occasional simultaneity of heating and dehumidification loads, employing a single reversible heat pump was deemed unfeasible. By applying the developed algorithm, which estimates the variability of the COP based on part load factor, heat pump size, and external temperature, all thermal loads have been converted into corresponding electrical loads. This process enabled the estimation of the specific electrical energy consumption (SEEC) for all the studied scenarios.

Most of the considerations discussed regarding the thermal loads can be directly extended to the electrical loads, given the evident correlation between the two. However, it is noteworthy that, from a SEEC perspective, locating a VF in a colder climate proved to be more advantageous. Specifically, the same VF situated in Shanghai and Dubai exhibited an increase in SEC of 2.55% and 5.66%, respectively, compared to the VF located in Trondheim. These differences become even more pronounced when considering the SEEC,

with increases of 7.8% and 8.14% for Shanghai and Dubai, respectively. This trend is primarily due to the fact that the cooling load represents the second largest energy demand in the system, following lighting. Consequently, the chiller heat pumps operate more efficiently in colder environments, such as Trondheim, where lower external temperatures improve their performance and reduce the cooling load compared to warmer climates like Shanghai and Dubai.

The increase in COP due to colder climates is less pronounced than initially expected. For the same VF scenario, the cooling heat pump achieved COP values of 4.49 in Trondheim, 4.28 in Shanghai, and 3.56 in Dubai. The relatively small difference between Trondheim and Shanghai is attributed to the condenser temperature limitations implemented by manufacturers to avoid off-design compressor operation.

For these reasons, as illustrated in Figure 9, the impact of the external climate on SEEC remains relatively limited. Removing the insulation layer generally leads to an increase in SEEC; however, this effect is partially mitigated by the use of heat pump. Since the COP for heating is typically higher than that for cooling, and the heating heat pump often operates in part load conditions, further improving its COP, the resulting increase in SEEC due to the absence of insulation is reduced. As a result, the SEEC increase is contained to approximately +8% in Trondheim and +5.2% in Dubai. Given the minimal difference observed between Trondheim and Shanghai, only SEEC values for Trondheim and Dubai have been presented in Figure 9 to facilitate a clearer comparison. Similarly to SEC, the most energy-efficient scenario is represented by T\_I\_100\_24\_1400, achieving a SEEC of 5.05 kWh<sub>el</sub> kg<sup>-1</sup>.

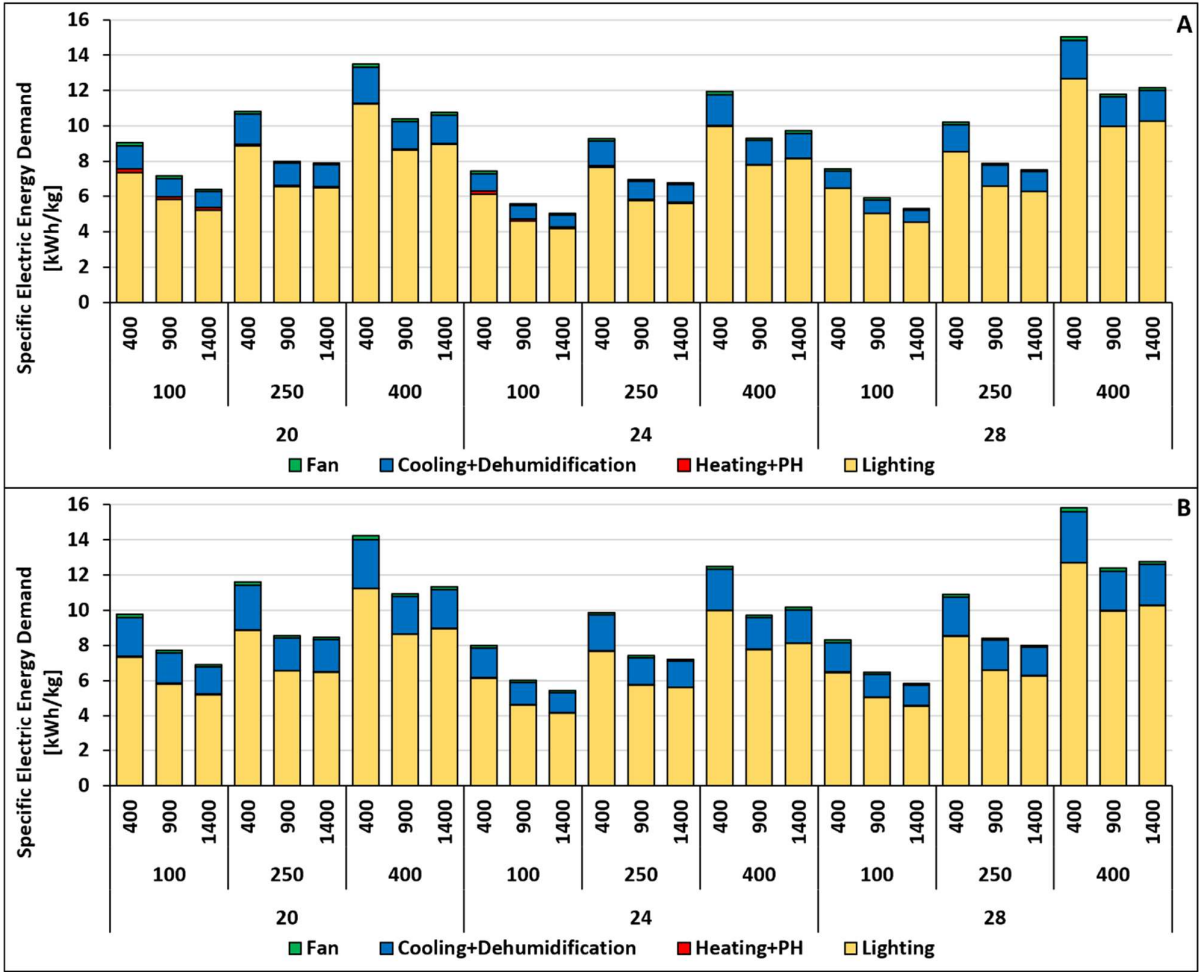


Figure 9: *Specific Electric Energy Consumption of the VF under two simulated locations: (A) Trondheim, (B) Dubai.*

### 3.6. Economic Assessments

Knowing the size of all the major components within the vertical farming system, the capital expenditure (CAPEX) for each scenario was calculated. Since the costs of all components are assumed to be independent of the VF's geographical location, only the CAPEX for the Trondheim site is shown in Figure 10. The cost of the carbon fertilization system was considered negligible, so Figure 10 illustrates only the influence of indoor temperature and PPF on the CAPEX.

Even from an economic perspective, it is noteworthy that the HVACD system contributes a relatively modest portion, representing approximately 14% of the total CAPEX. The cost of the growing chamber is fixed, as it depends solely on the net growing area, and accounts for 19 to 41% of the capital investment. It is important to note that the building is assumed to be pre-existing and used under a lease agreement; therefore, construction costs are not included.

As with the energy-related results, the lighting system represents the most significant share of the capital costs, ranging from 35 to 55%. This includes future replacement expenses, as LEDs are the component with the shortest operational lifespan. Considering all simulated scenarios, the total CAPEX for a vertical farm is

estimated to range between 61.0 and 140.0 thousand dollars, resulting in a specific cost of approximately 680 to 1560 \$ per square meter of cultivated area.

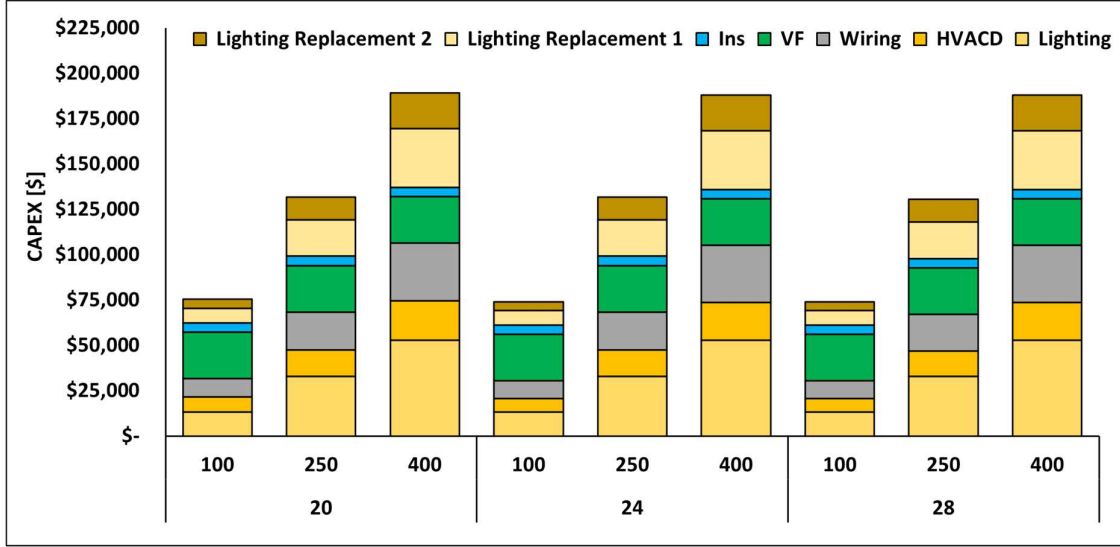


Figure 10: *Capital Expenditures of the well-insulated VF as a function of indoor conditions (Temperature and PPFD).*

The operational expenditure, which includes annual costs for water, CO<sub>2</sub>, electricity, labor, and leasing, was evaluated for each considered location in order to highlight the differences (see Figure 11). It is important to note that, in all scenarios, labor costs represent the largest portion of the annual expenses of the vertical farm, accounting for approximately 25% in Shanghai, 39% in Trondheim, and 35% in Dubai.

Due to variations in cost of living, such as leasing rates and salaries, Shanghai results as the most cost-efficient location among those analyzed in this study for implementing vertical farming, with an annual OPEX ranging from 11 to 34 k\$. Under identical indoor conditions, the corresponding values for Trondheim and Dubai are 38 to 72% and 65 to 90% higher, respectively.

Because of the high energy demand required by vertical farming systems, the portion of OPEX related to electricity reaches about 12% when the light intensity is low and up to 19% when it is high, in the case of Trondheim. Although these values may vary slightly across locations, the general order of magnitude remains consistent.

Lastly, the contributions of carbon dioxide and water to the operational costs are minimal. The high water use efficiency achieved by the system significantly limits the need for external water supply, resulting in a nearly negligible cost for water.

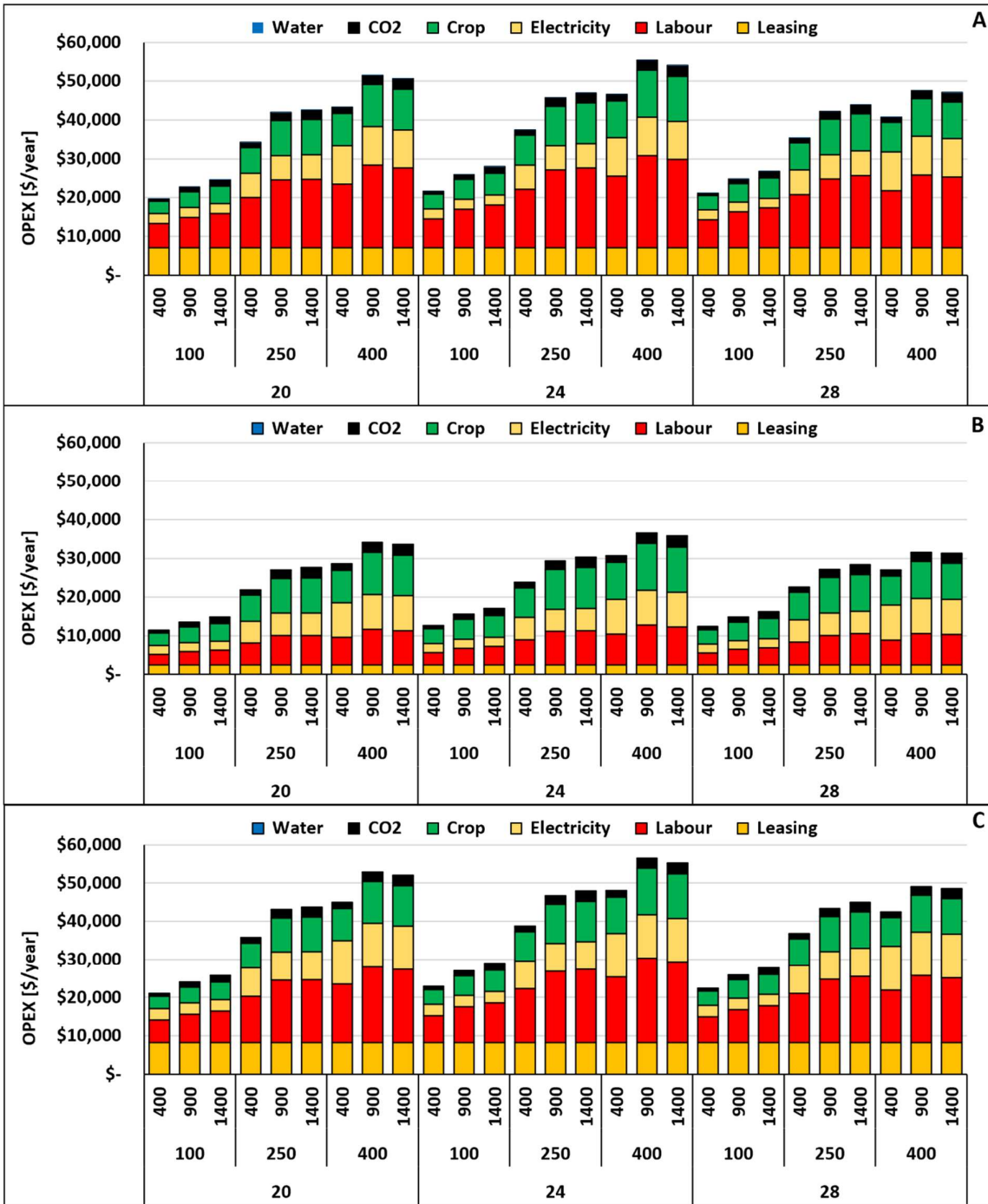


Figure 11: Operational Expenditures of the well-insulated VF as a function of indoor conditions (Temperature, PPF, and CO<sub>2</sub> concentration) in three simulated locations: (A) Trondheim, (B) Dubai.

To present the overall results of the economic assessment, the levelized cost of lettuce for each insulated scenario is illustrated in Figure 12. The trend of the LCoL remains consistent across all studied locations, as the productivity of the vertical farm is not influenced by external climatic conditions. As anticipated from the CAPEX and OPEX evaluations, the LCoL values for the vertical farm located in Shanghai are significantly lower than those observed in Trondheim and Dubai.

The CO<sub>2</sub> prices considered resulted in lower LCoL values in scenarios where higher CO<sub>2</sub> concentrations led to increased crop productivity. For example, at a PPFD of 250 μmol m<sup>-2</sup> s<sup>-1</sup>, a 12% increase in CO<sub>2</sub> cost would make the 900 ppm and 1400 ppm concentrations equally cost-effective. However, in that same scenario, the CO<sub>2</sub> price would need to be approximately four and a half times higher to render carbon fertilization economically unviable. This threshold decreases at higher PPFD levels, while it increases at lower PPFD levels.

Instead, the electricity price directly influences the tradeoff between the higher productivity and the higher energy consumption, both of which are associated with increasing the PPFD level. With the selected electricity price, the assessment showed that the lowest LCoL was achieved by setting an intermediate PPFD of 250 μmol m<sup>-2</sup> s<sup>-1</sup> across all studied locations. Specifically, in Trondheim, if the electricity price were reduced by 41% (to 0.059 \$ kWh<sup>-1</sup>), the 400 μmol m<sup>2</sup> s<sup>-1</sup> scenario would become as cost-effective as the intermediate one. Conversely, if the electricity price increased by 123% (to 0.223 \$ kWh<sup>-1</sup>), the 100 μmol m<sup>2</sup> s<sup>-1</sup> scenario would become competitive. Table 5 summarizes this analysis for each indoor temperature and location evaluated, assuming a CO<sub>2</sub> concentration of 900 ppm. The terms C<sub>el400</sub> and C<sub>el100</sub> refer to the electricity prices required to make the high and low PPFD scenarios, respectively, as viable as the intermediate one.

Based on the presented results, the most cost-effective scenarios among those analyzed in this study are T\_I\_250\_24\_1400, S\_I\_250\_24\_1400, and D\_I\_250\_24\_1400, achieving a LCoL of 6.38, 4.57, and 6.48 \$ kg<sup>-1</sup>, respectively. It is noteworthy that, with an installation cost of 5.1 k\$, the insulation layer slightly increases the LCoL when compared with the corresponding uninsulated scenario. In a cold climate such as Trondheim, if the insulation cost rises by more than 35%, the uninsulated scenario becomes more cost-effective. A similar analysis in a hot climate, such as Dubai, shows that a cost increase of only 20% would make the insulated configuration less economically favorable. This difference is influenced not only by the external climate but also by other location-dependent expenses, including leasing, labor, and electricity.

Table 5: *Electricity price variations required to improve the competitiveness of high-PPFD scenarios.*

<b>Location</b>	<b>Temperature</b>	<b>C<sub>el400</sub> [\$ kWh<sup>-1</sup>]</b>	<b>C<sub>el100</sub> [\$ kWh<sup>-1</sup>]</b>
	[°C]		
Trondheim	20	0.067 (-33%)	0.285 (+185%)
	24	0.059 (-41%)	0.223 (+123%)
	28	0.026 (-74%)	0.198 (+98%)
Shanghai	20	0.052 (-42%)	0.188 (+109%)
	24	0.045 (-50%)	0.143 (+59%)
	28	0.017 (-81%)	0.125 (+39%)
Dubai	20	0.080 (-27%)	0.306 (+178%)
	24	0.072 (-35%)	0.244 (+122%)
	28	0.036 (-67%)	0.218 (+98%)

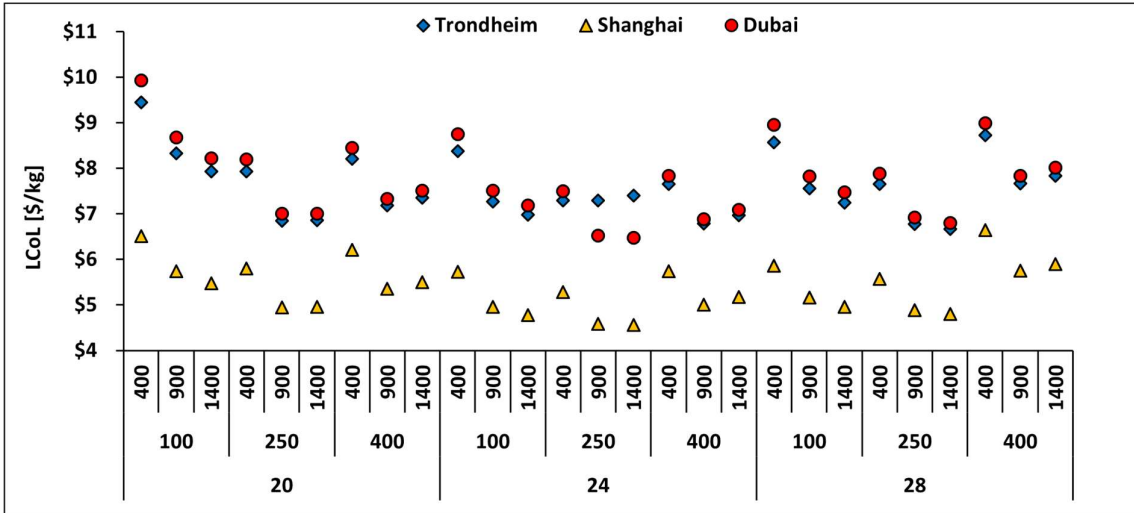


Figure 12: *Levelized cost of lettuce for a well-insulated VF under varying indoor conditions and external socio-environmental settings.*

### 3.7. Sustainability Assessment

After evaluating the vertical farm's performance from agricultural, energy, and economic perspectives, it is important to assess its sustainability by comparing vertically grown lettuce with imported lettuce. Since the previous section identified the most cost-effective scenarios, these have been selected for comparison in terms of CO<sub>2</sub> equivalent emissions with those associated with an equivalent quantity of imported lettuce.

In this analysis, only the emissions associated with the energy demand of the vertical farm have been considered. Figure 13 illustrates the carbon footprint savings of vertically grown lettuce compared to imported lettuce across the three studied locations. These savings are primarily influenced by the local energy mix and the characteristics of the supply chain. Under current conditions, it becomes evident that highly energy-intensive vertical farms can only be considered environmentally sustainable in regions where the share of renewable energy in the grid is substantial. In Norway, where hydropower and wind energy account for 89% and 9% of the energy mix, respectively, vertical farming achieves a carbon reduction of 230 grams of CO<sub>2</sub> per kilogram of lettuce. This corresponds to a 70% decrease in emissions compared to the import alternative.

In Shanghai and Dubai, the high emission factors associated with electricity consumption make vertical farming significantly unsustainable from a carbon footprint perspective. Adopting solutions with lower light intensity would improve the sustainability of vertical farming in these contexts by reducing emissions by 60 percent when switching the PPF from 250 to 100  $\mu\text{mol m}^{-2} \text{s}^{-1}$ . Due to China's high emission factor and the potentially short supply chain, an improvement in energy efficiency of 98.8% would be necessary to make vertical farming sustainable. In Dubai, where the supply chain is more emission-intensive, this required efficiency improvement is reduced to 62%.

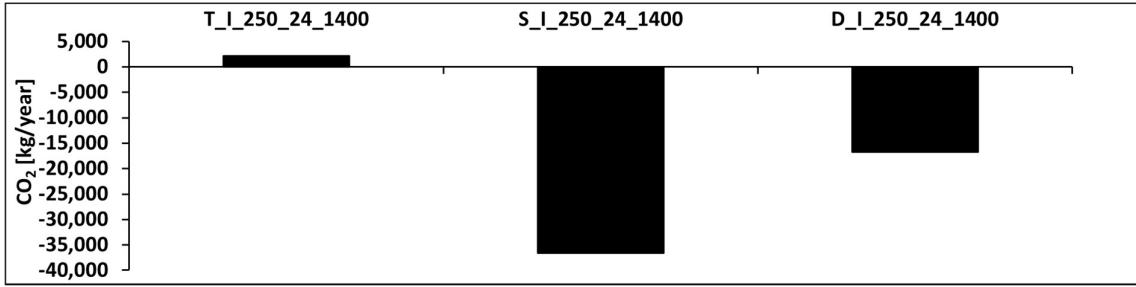


Figure 13: Estimated CO<sub>2</sub> emission savings from local vertical farm (VF) lettuce production versus conventional supply chain alternatives.

### 3.8. Distance Correlation for the Economic Assessments

To finalize the assessments regarding the influence of each input variable on the investment requirements (CAPEX), operational costs, LCoL, and CO<sub>2</sub> emission savings, the results are summarized in Figure 14. As shown, indoor temperature and the presence of an insulation layer have a minimal effect on these key parameters. This is due to their limited impact on both the resource consumption and the crop production within the vertical farm system.

It is particularly interesting to note that, even though PPFD shows a correlation coefficient of 0.999 with CAPEX and 0.730 with OPEX, its impact on the LCoL is limited to 0.200. While CAPEX and OPEX are strongly influenced by PPFD because light intensity determines both the size of the HVACD system and the electricity consumption, its effect on LCoL is reduced due to the non-linear relationship with crop productivity.

On the other hand, the impact of carbon dioxide fertilization on crop growth is more direct and significant, resulting in a correlation coefficient of 0.327 with the LCoL and 0.448 with carbon emission savings. Additionally, CO<sub>2</sub> concentration significantly influences the operational expenditures of the VF, with a correlation coefficient of 0.222 with OPEX.

In this analysis, climate refers to both the external environmental conditions and the socio-economic context, as it influences certain expenses and the energy mix that determine the CO<sub>2</sub> savings of the vertical farm. The CAPEX is almost unaffected by climate, since it only alters the size of the HVACD system required to maintain the desired indoor environment. In contrast, differences in electricity prices, land leasing, and labor costs cause climate to have a significant effect on both the OPEX and the LCoL, with distance correlation coefficients of 0.496 and 0.734, respectively. Additionally, due to variations in supply chains, climate also plays a substantial role in determining CO<sub>2</sub> savings, reaching a distance correlation coefficient of 0.576.

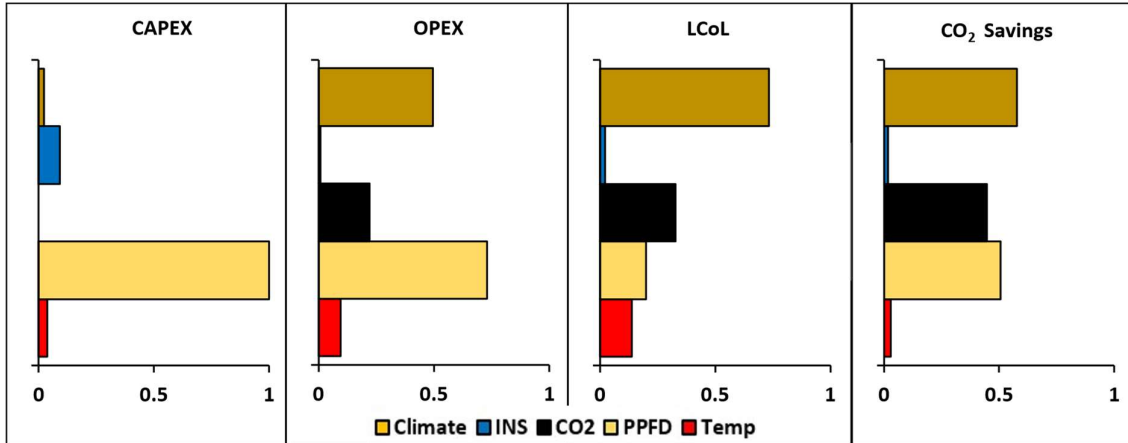


Figure 14: *Distance correlation coefficient of input parameters on economic and sustainability performance in vertical farming.*

#### 4. Conclusions

This paper presented the results of an extensive analysis aimed at identifying and quantifying the impact of parameters affecting the Controlled Environment Agriculture systems, specifically a hydroponic vertical farm designed for lettuce cultivation. Such impact is measured via key performance indicators such as energy consumption, water use efficiency, and the levelized cost of lettuce, with the goal of providing specific best practices for the development of future vertical farming systems worldwide.

All the annual resource requirements obtained by the employed transient model were subsequently integrated into the economic assessment to estimate both capital and operational costs, leading to the calculation of the levelized cost of lettuce for each scenario analyzed. Finally, different supply chain conditions were considered to compare the emissions associated with vertical farming production against those from importing an equivalent amount of lettuce.

To assess the influence of indoor conditions, insulation and VF's location on key performance indicators 162 one-year scenarios were run varying temperature, PPF, CO<sub>2</sub> concentration, insulation, and climate (Trondheim, Shanghai, Dubai) Distance correlation coefficients, were used to quantify each parameter's impact.

The main conclusions of this analysis are summarised as follows:

- The HVACD system ensured stable crop productivity in VFs despite varying external climate conditions. PPF was identified as the primary driver of crop growth ( $\rho = 0.85$ ), followed by CO<sub>2</sub> concentration ( $\rho = 0.36$ ) and indoor temperature ( $\rho = 0.22$ ). While the highest productivity was achieved at a PPF of 400  $\mu\text{mol m}^{-2} \text{s}^{-1}$ , LUE decreased at higher PPF, making it essential to balance productivity with energy costs. CO<sub>2</sub> fertilization showed a saturation trend, with 900 ppm identified as an effective threshold. An indoor temperature of 24°C is recommended for optimal lettuce cultivation.
- PPF also emerged as the primary driver of the VF's total energy load ( $\rho = 0.73$ ) influencing both lighting and HVACD demands. The most energy-efficient condition occurred at a low PPF of 100  $\mu\text{mol m}^{-2} \text{s}^{-1}$ , where LUE was higher and CO<sub>2</sub> enhancement more effective. However, this scenario also resulted in lowest specific

productivity ( $55 \text{ kg m}^{-2}$ ). Thus, selecting the optimal PPFD level requires balancing energy efficiency and crop yield.

- In cold climates, under PPFD conditions, the absence of an insulation layer can reduce the SEC by up to 5%, as heat losses through the envelope help offset the cooling load. However, at low PPFD, the need for additional heating leads to a significant SEC increase (40-70%), worsening energy performance. In hot climates, removing insulation consistently raised SEC (by 1-21%) with no energy benefits. Still, high PPFD and elevated indoor temperatures can partially mitigate these negative effects.
- Given the trade-off between energy use and productivity, the LCoL emerges as the key parameter for identifying optimal operating conditions. The lowest LCoL across all climates was achieved with a temperature of  $24^\circ\text{C}$ , PPFD of  $250 \mu\text{mol m}^{-2} \text{ s}^{-1}$ , CO<sub>2</sub> concentration of 1400 ppm, and the presence of an insulation layer. Under these conditions, the resulting LCoL ranged from  $4.57$  to  $6.48 \text{ \$ kg}^{-1}$  depending on the location.
- Electricity price also significantly affected LCoL ( $\rho = 0.22$ ). A reduction in electricity prices by 35-50% would make high-PPFD, high-productivity scenarios more economically viable. While insulation had only a minor impact on LCoL in optimal scenarios ( $1$  to  $3 \text{ c\$ kg}^{-1}$ ), its adoption may be reconsidered if installation costs exceed the study's reference values by 20-35%, at which point energy savings no longer justify the expense.
- Finally, due to the high energy demand of vertical farming, its carbon footprint is highly sensitive to the local energy mix ( $\rho = 0.58$ ). Currently, only countries with near-complete energy decarbonization, such as Norway, can support vertical farming without increasing CO<sub>2</sub> emissions compared to conventional lettuce imports.
- Notably, in hot and arid climates, vertical farms achieved higher WUE due to the moisture condensation from the incoming air within the HVACD system. This process may significantly reduce water demand in regions where freshwater is scarce and would otherwise require energy-intensive desalination for greenhouse farming. The authors highlight this as a promising area for further research, given its potential to lower the overall CO<sub>2</sub> emissions.

## 5. Appendix and supplementary data

### 5.1 Distance Correlation Coefficient Methodology

The distance correlation coefficient ( $\rho$ ) is a statistical measure used to evaluate the dependence between two different variables, X and Y, by comparing the similarities between their respective distance matrices, A and B. Let  $x_{i,j}$  and  $y_{i,j}$  represent the values taken by variables X and Y. The generic distance matrices  $D_{ij}$  are defined as shown in Eqs. A1 and A2. Both matrices have dimensions  $n \times n$ , where  $n$  refers to the number of observations, which in this study corresponds to the number of evaluated scenarios (162).

$$D_{ij}^X = |x_i - x_j| \quad (\text{A1})$$

$$D_{ij}^Y = |y_i - y_j| \quad (\text{A2})$$

Each distance matrix has been centered using a double centering operation, as described in Eqs. A3 and A4. In this process,  $\bar{D}_{i\cdot}$ ,  $\bar{D}_{\cdot j}$ ,  $\bar{D}_{\cdot \cdot}$  represent the average values calculated across the i-th row, the j-th column, and the entire matrix, respectively.

$$A_{ij} = \bar{D}_{ij}^X - \bar{D}_{i\cdot}^X - \bar{D}_{\cdot j}^X + \bar{D}_{\cdot \cdot}^X \quad (\text{A3})$$

$$B_{ij} = \bar{D}_{ij}^Y - \bar{D}_{i\cdot}^Y - \bar{D}_{\cdot j}^Y + \bar{D}_{\cdot \cdot}^Y \quad (\text{A4})$$

These matrices have ultimately been used to determine the covariance between X and Y, as well as the individual variances of the two selected variables, as expressed in Eqs. A5, A6, and A7. These expressions were employed in the equation reported in the methodology section.

$$dCov^2(X, Y) = \frac{1}{n^2} \sum_{i=1}^n \sum_{j=1}^n A_{ij} B_{ij} \quad (\text{A5})$$

$$dVar^2(X) = \frac{1}{n^2} \sum_{i=1}^n \sum_{j=1}^n A_{ij} A_{ij} \quad (\text{A6})$$

$$dVar^2(Y) = \frac{1}{n^2} \sum_{i=1}^n \sum_{j=1}^n B_{ij} B_{ij} \quad (\text{A6})$$

## 5.2 Thermal Load of Insulated Vertical Farms

This section presents the thermal load trends for all simulated scenarios, enabling comparison between them and highlighting the impact of climate, PPFD, and temperature on the thermal load when the building is well insulated. It is noteworthy that in all scenarios the heating load decreases as the external climate becomes warmer. Additionally, as PPFD increases, the cooling load rises significantly, while the dehumidification load becomes nearly negligible.

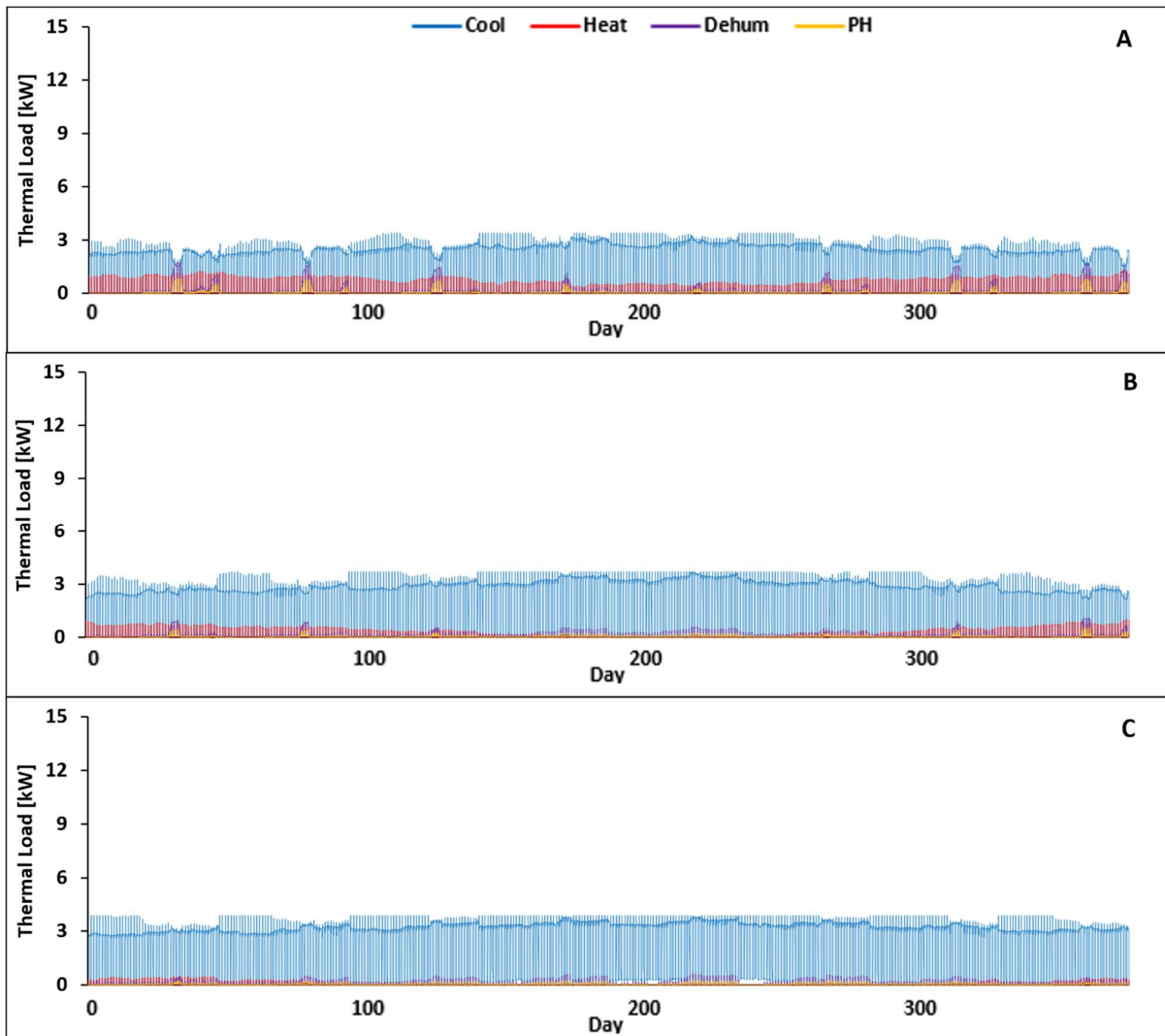
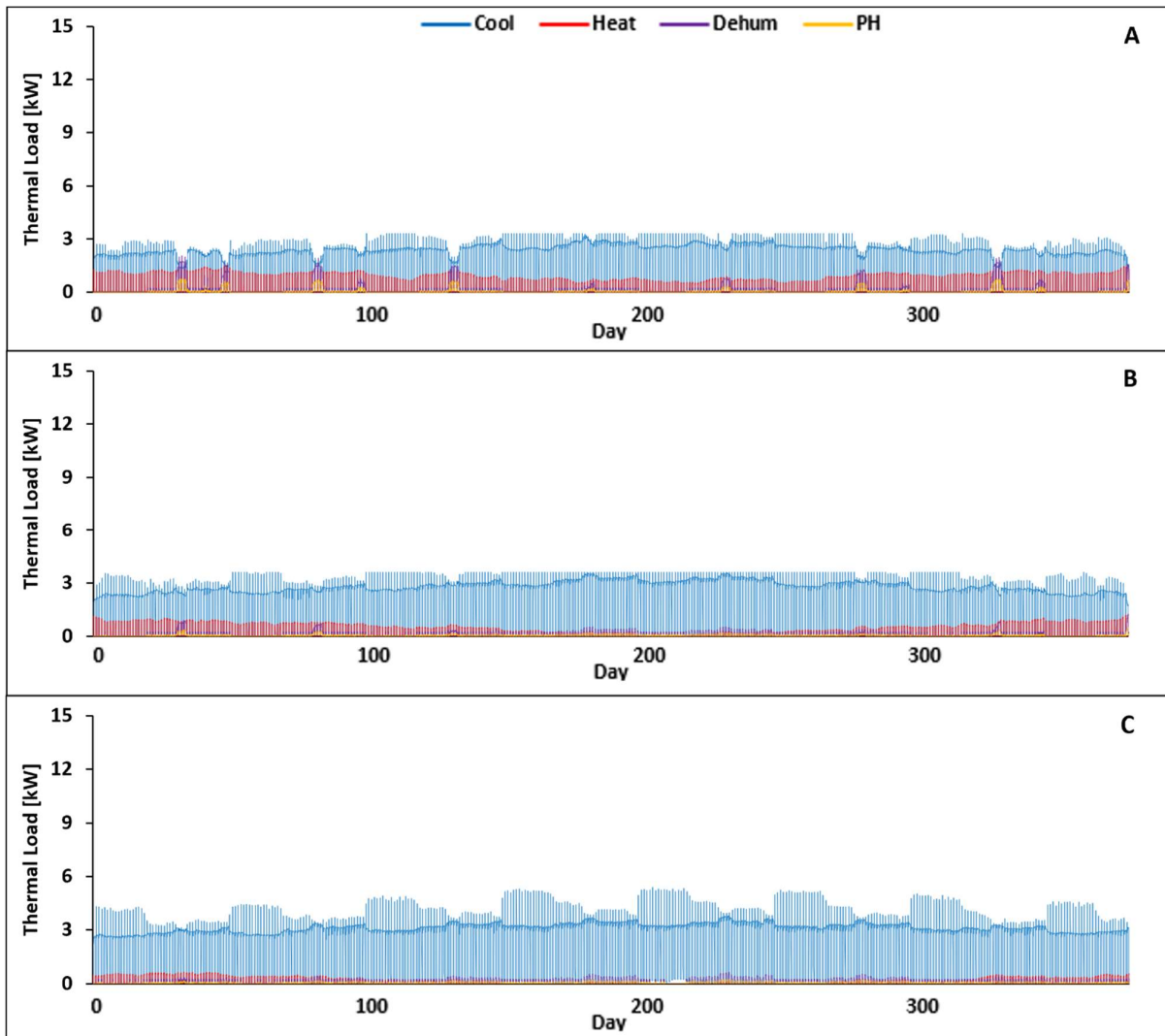


Figure A1: Heating, cooling, dehumidification and post-heating loads throughout the year for a well-insulated VF in three locations: (A) Trondheim, (B) Shanghai, (C) Dubai. The results were obtained under conditions of 24 °C and 100  $\mu\text{mol m}^{-2} \text{s}^{-1}$ .



*Figure A2: Heating, cooling, dehumidification and post-heating loads throughout the year for a well-insulated VF in three locations: (A) Trondheim, (B) Shanghai, (C) Dubai. The results were obtained under conditions of 28 °C and 100  $\mu\text{mol m}^{-2} \text{s}^{-1}$ .*

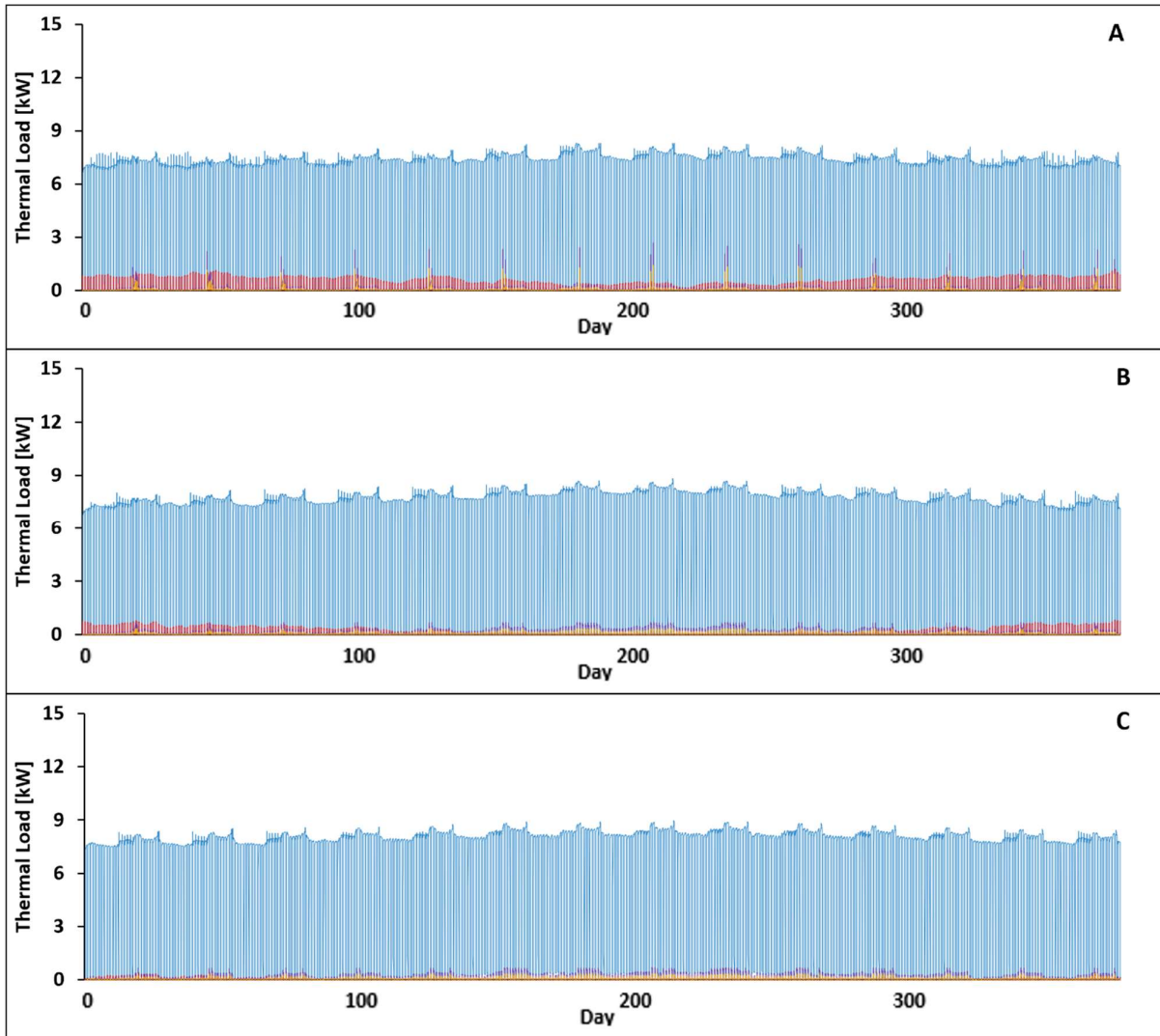


Figure A3: Heating, cooling, dehumidification and post-heating loads throughout the year for a well-insulated VF in three locations: (A) Trondheim, (B) Shanghai, (C) Dubai. The results were obtained under conditions of 20 °C and 250  $\mu\text{mol m}^{-2} \text{s}^{-1}$ .

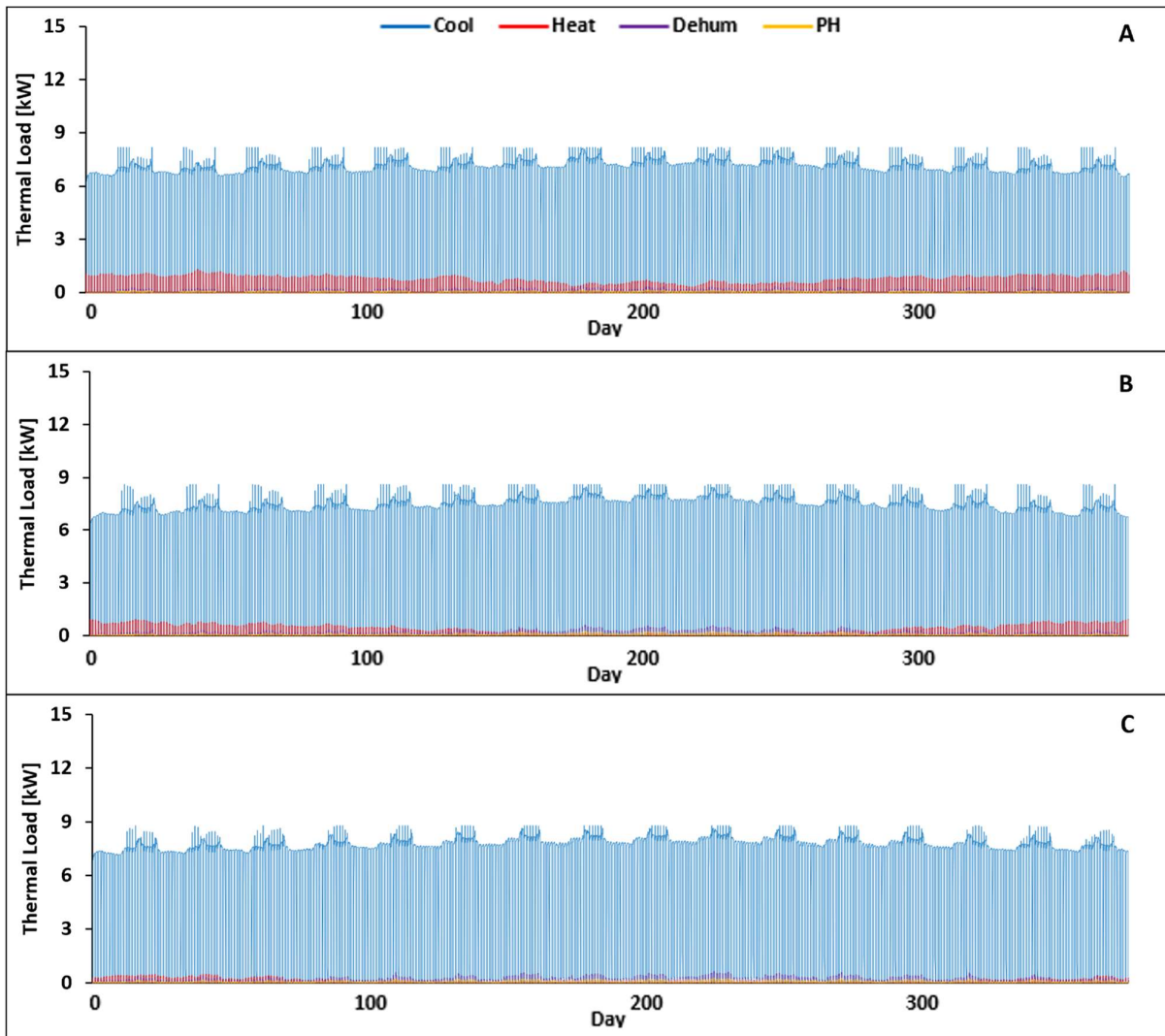
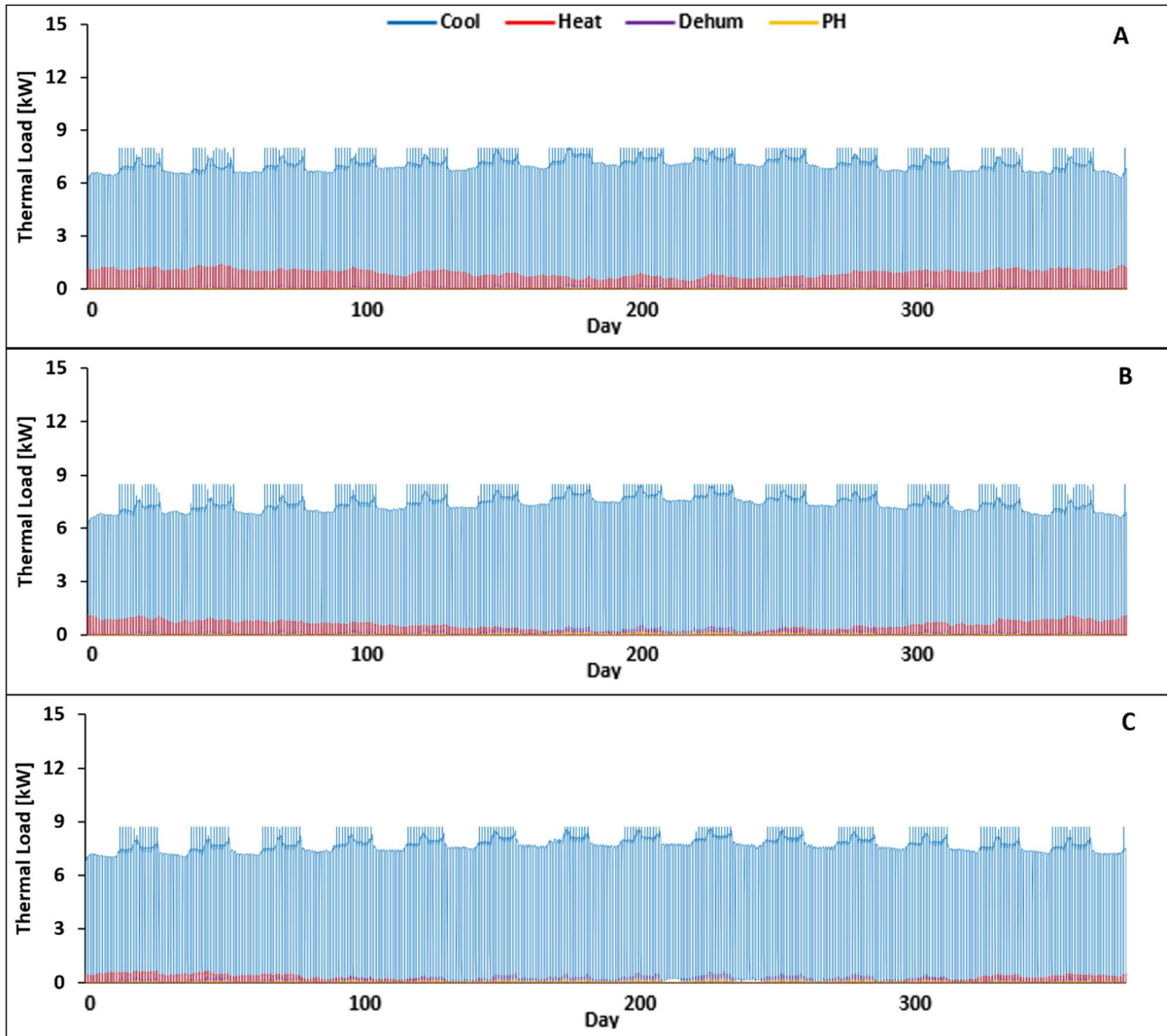


Figure A4: Heating, cooling, dehumidification and post-heating loads throughout the year for a well-insulated VF in three locations: (A) Trondheim, (B) Shanghai, (C) Dubai. The results were obtained under conditions of 24 °C and 250  $\mu\text{mol m}^{-2} \text{s}^{-1}$ .



*Figure A5: Heating, cooling, dehumidification and post-heating loads throughout the year for a well-insulated VF in three locations: (A) Trondheim, (B) Shanghai, (C) Dubai. The results were obtained under conditions of 28 °C and 250  $\mu\text{mol m}^{-2} \text{s}^{-1}$ .*

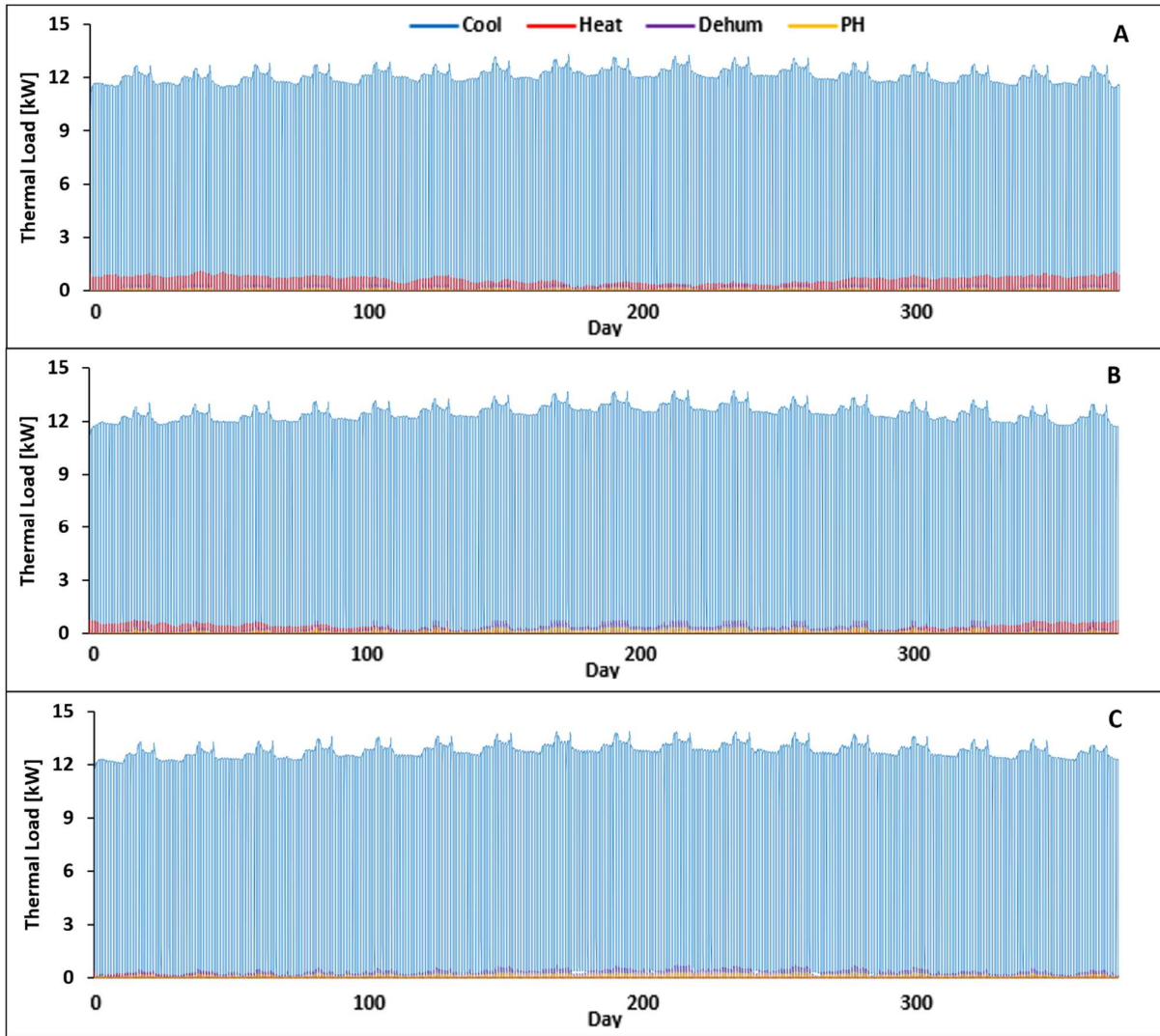
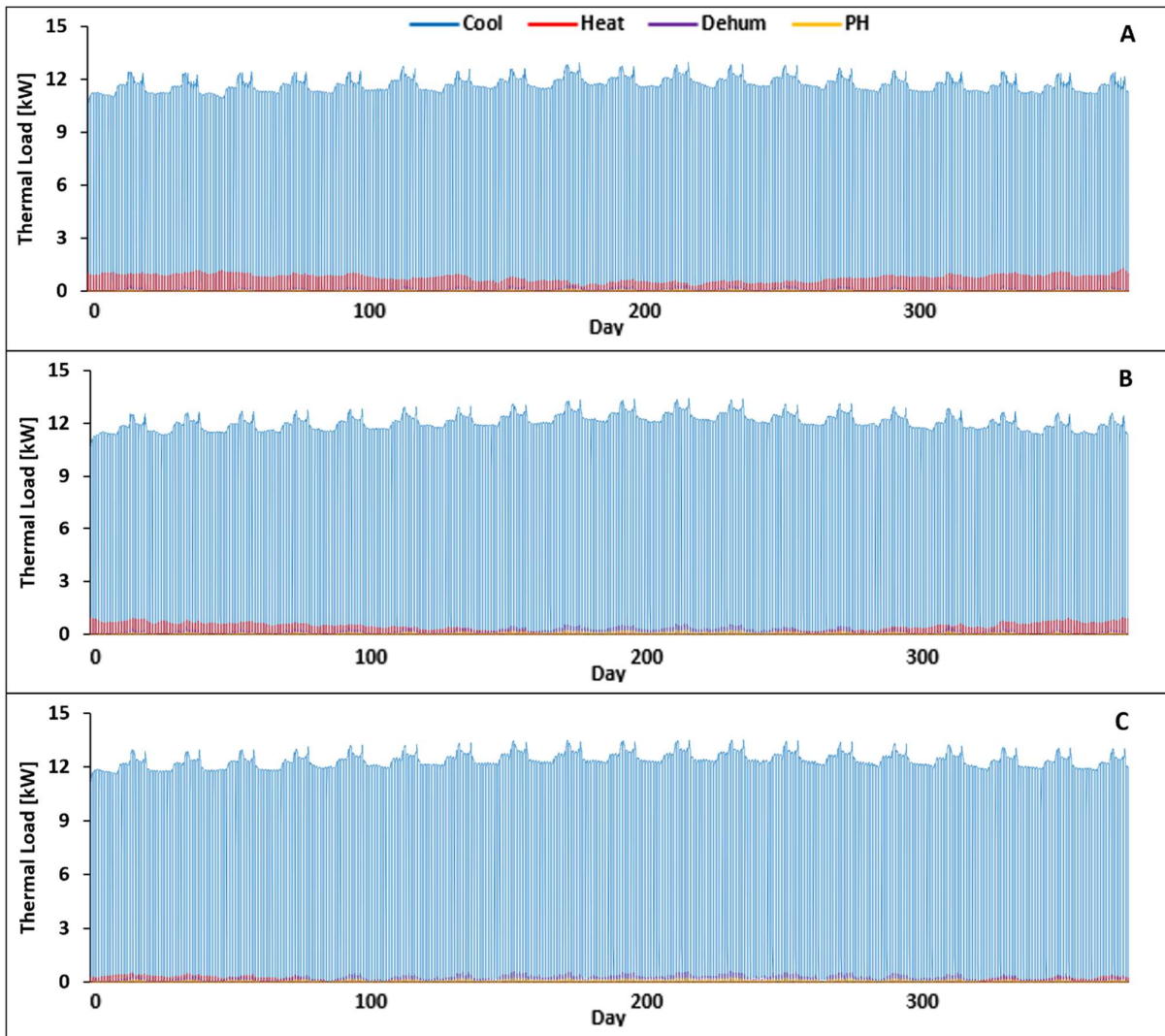
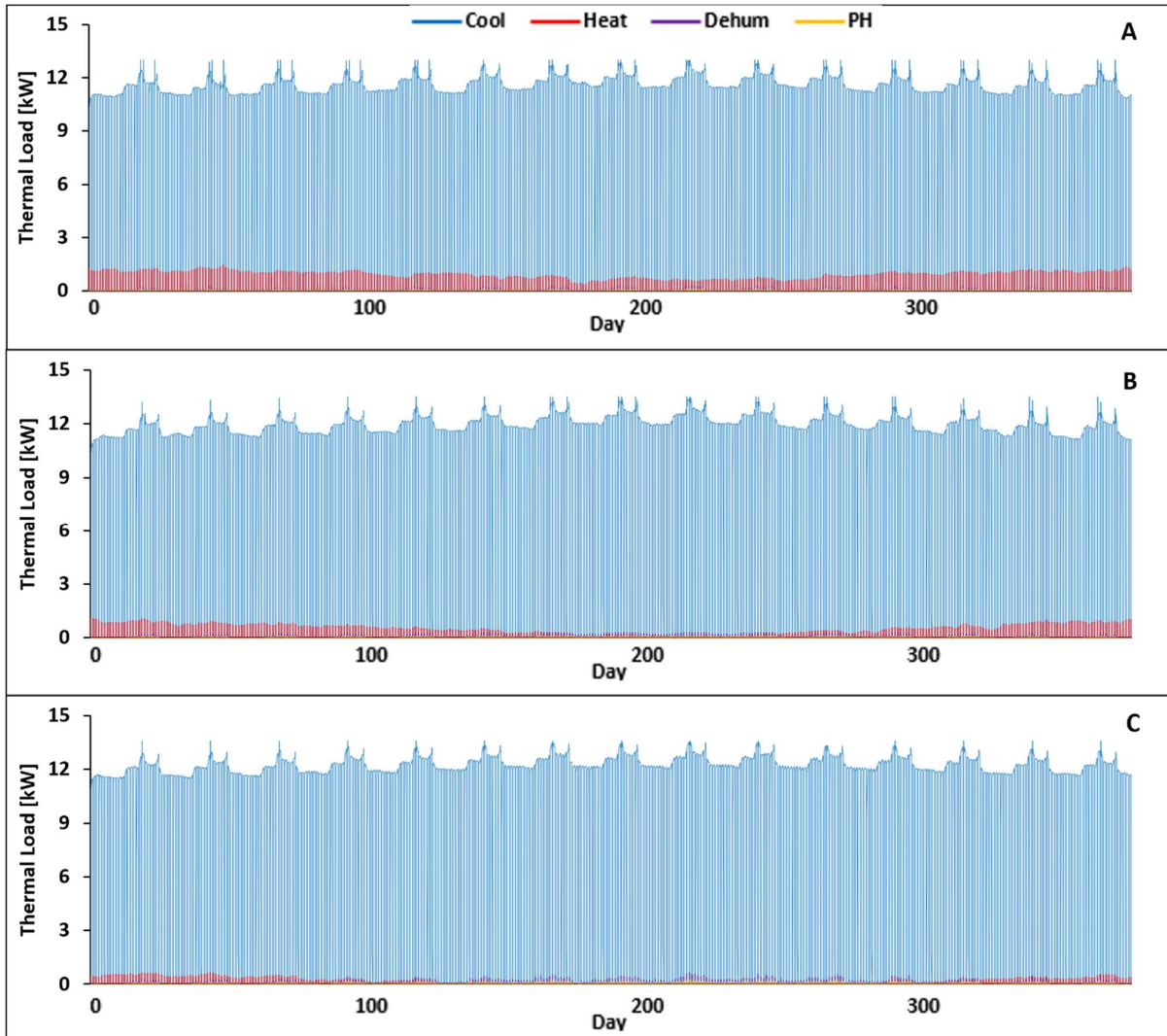


Figure A6: Heating, cooling, dehumidification and post-heating loads throughout the year for a well-insulated VF in three locations: (A) Trondheim, (B) Shanghai, (C) Dubai. The results were obtained under conditions of 20 °C and 400  $\mu\text{mol m}^{-2} \text{s}^{-1}$ .



*Figure A7: Heating, cooling, dehumidification and post-heating loads throughout the year for a well-insulated VF in three locations: (A) Trondheim, (B) Shanghai, (C) Dubai. The results were obtained under conditions of 24 °C and 400  $\mu\text{mol m}^{-2} \text{s}^{-1}$ .*



*Figure A8: Heating, cooling, dehumidification and post-heating loads throughout the year for a well-insulated VF in three locations: (A) Trondheim, (B) Shanghai, (C) Dubai. The results were obtained under conditions of 28 °C and 400  $\mu\text{mol m}^{-2} \text{s}^{-1}$ .*

### 5.3 Thermal Load of Not-Insulated Vertical Farm

This section presents the thermal load trends for all simulated scenarios without the insulation layer. The observations made in the previous section also apply to these non-insulated scenarios.

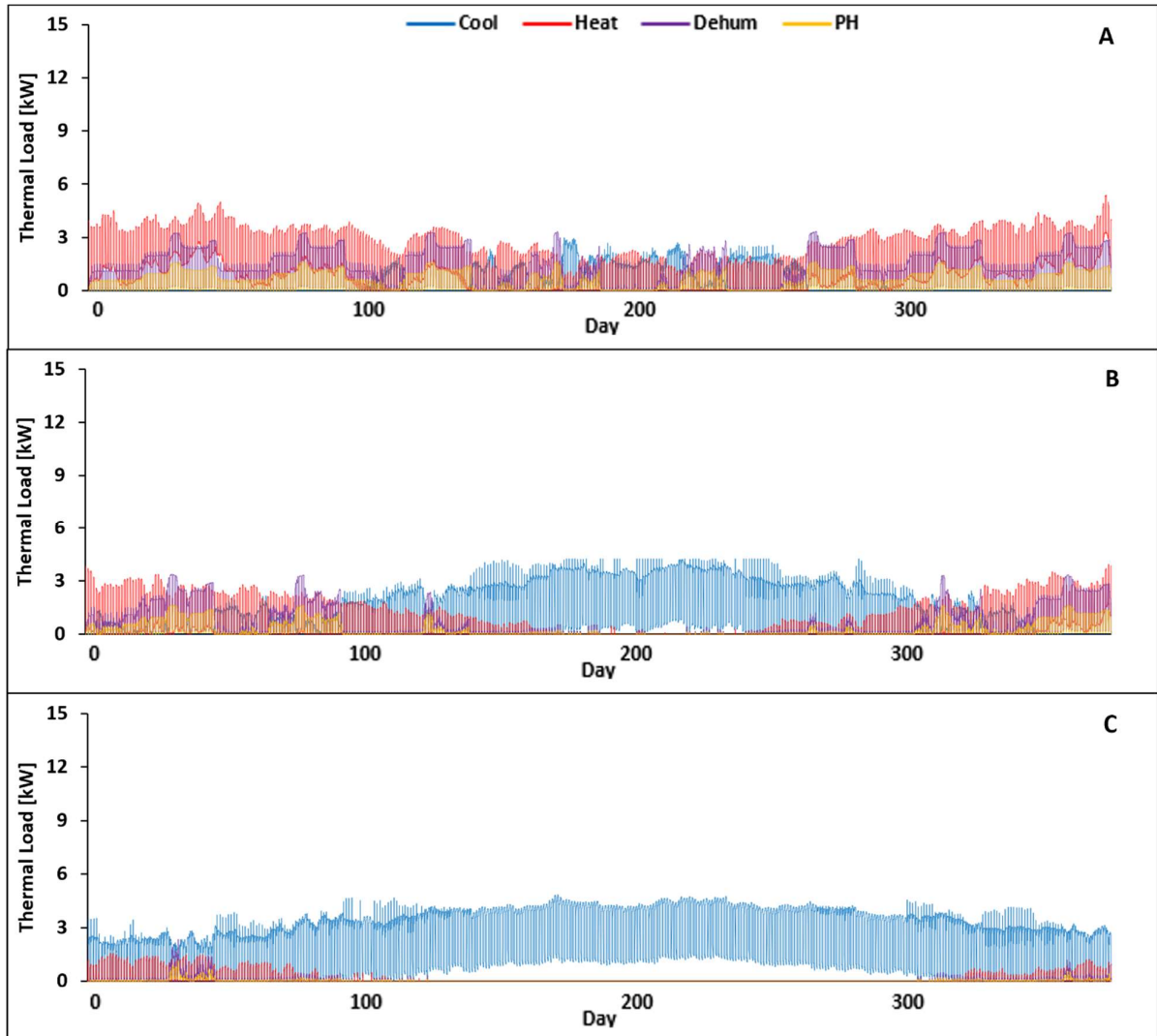


Figure A9: Heating, cooling, dehumidification and post-heating loads throughout the year for a not-insulated VF in three locations: (A) Trondheim, (B) Shanghai, (C) Dubai. The results were obtained under conditions of 24 °C and 100  $\mu\text{mol m}^{-2} \text{s}^{-1}$ .

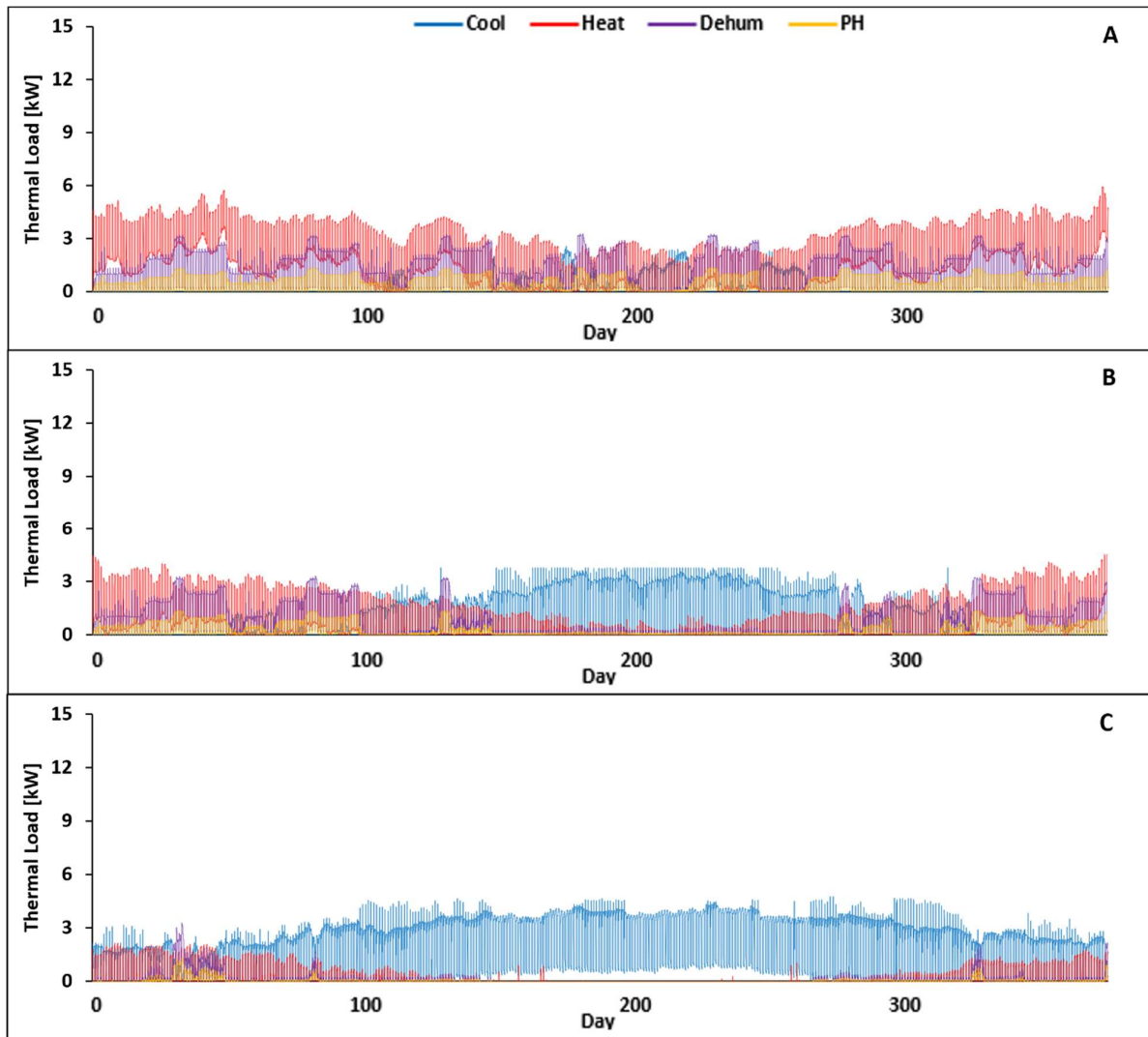


Figure A10: Heating, cooling, dehumidification and post-heating loads throughout the year for a not-insulated VF in three locations: (A) Trondheim, (B) Shanghai, (C) Dubai. The results were obtained under conditions of 28 °C and 100  $\mu\text{mol m}^{-2} \text{s}^{-1}$ .

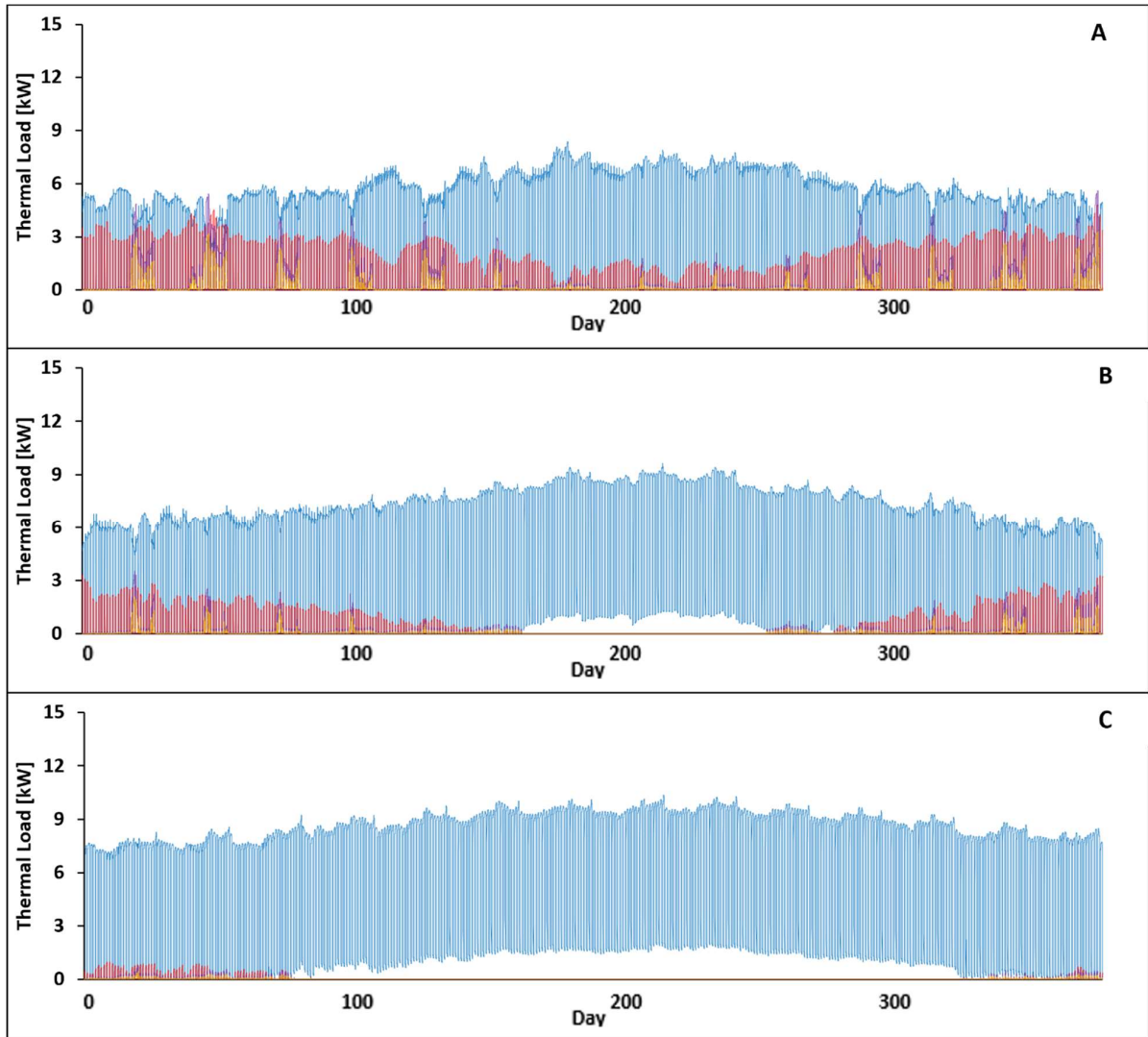


Figure A11: Heating, cooling, dehumidification and post-heating loads throughout the year for a not-insulated VF in three locations: (A) Trondheim, (B) Shanghai, (C) Dubai. The results were obtained under conditions of 20 °C and 250  $\mu\text{mol m}^{-2} \text{s}^{-1}$ .

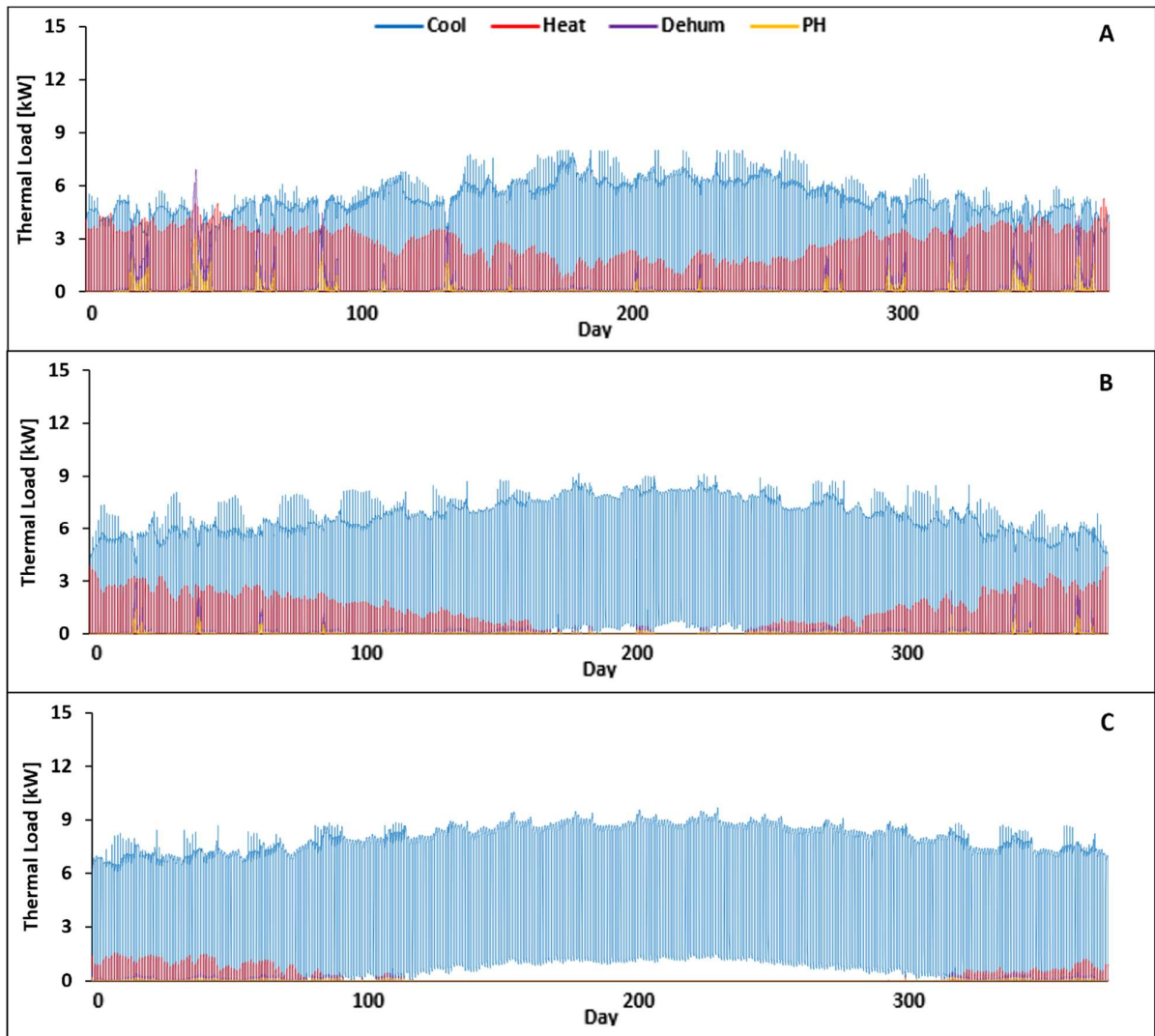


Figure A12: Heating, cooling, dehumidification and post-heating loads throughout the year for a not-insulated VF in three locations: (A) Trondheim, (B) Shanghai, (C) Dubai. The results were obtained under conditions of 24 °C and 250  $\mu\text{mol m}^{-2} \text{s}^{-1}$ .

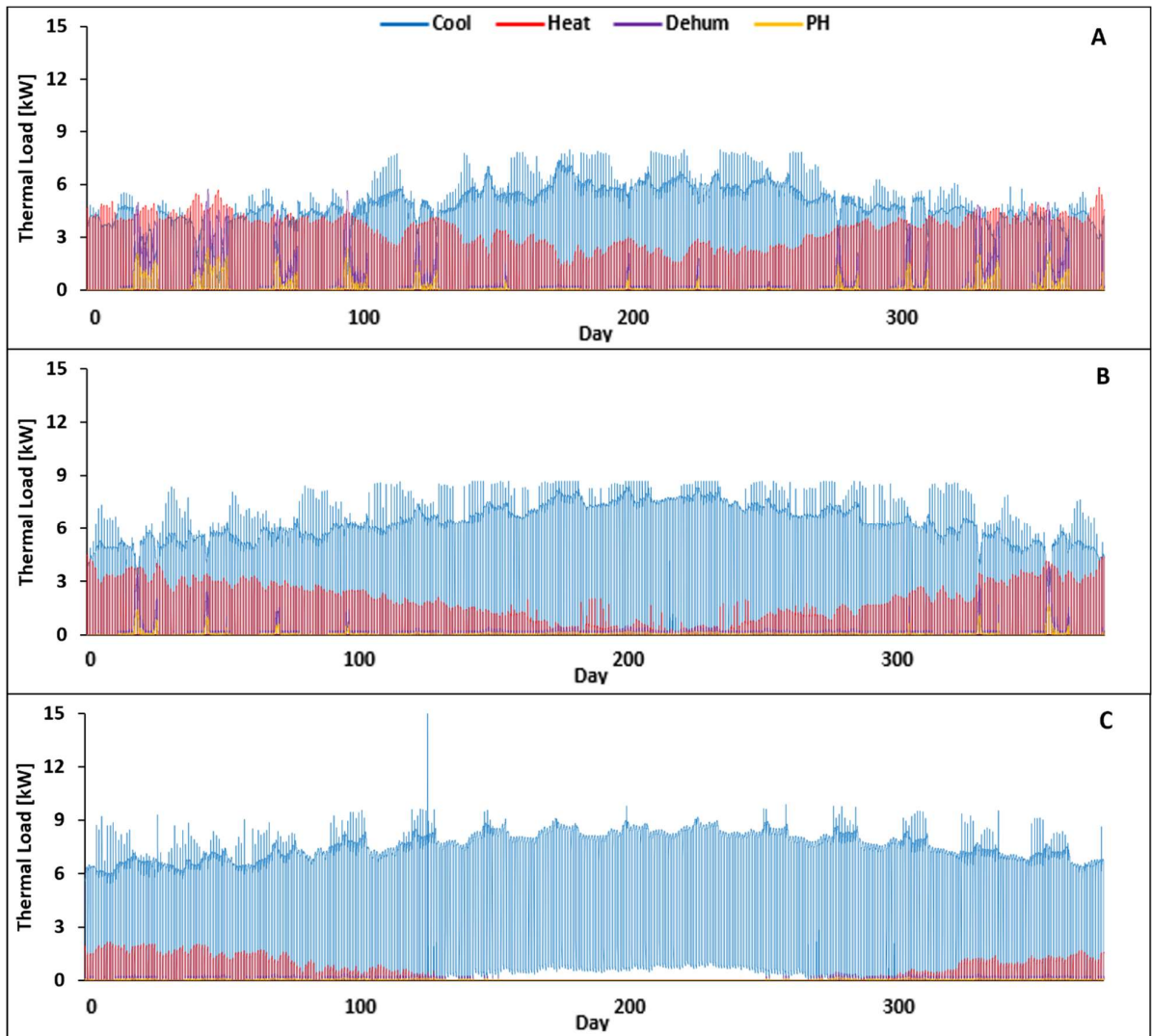


Figure A13: Heating, cooling, dehumidification and post-heating loads throughout the year for a not-insulated VF in three locations: (A) Trondheim, (B) Shanghai, (C) Dubai. The results were obtained under conditions of 28 °C and 250  $\mu\text{mol m}^{-2} \text{s}^{-1}$ .

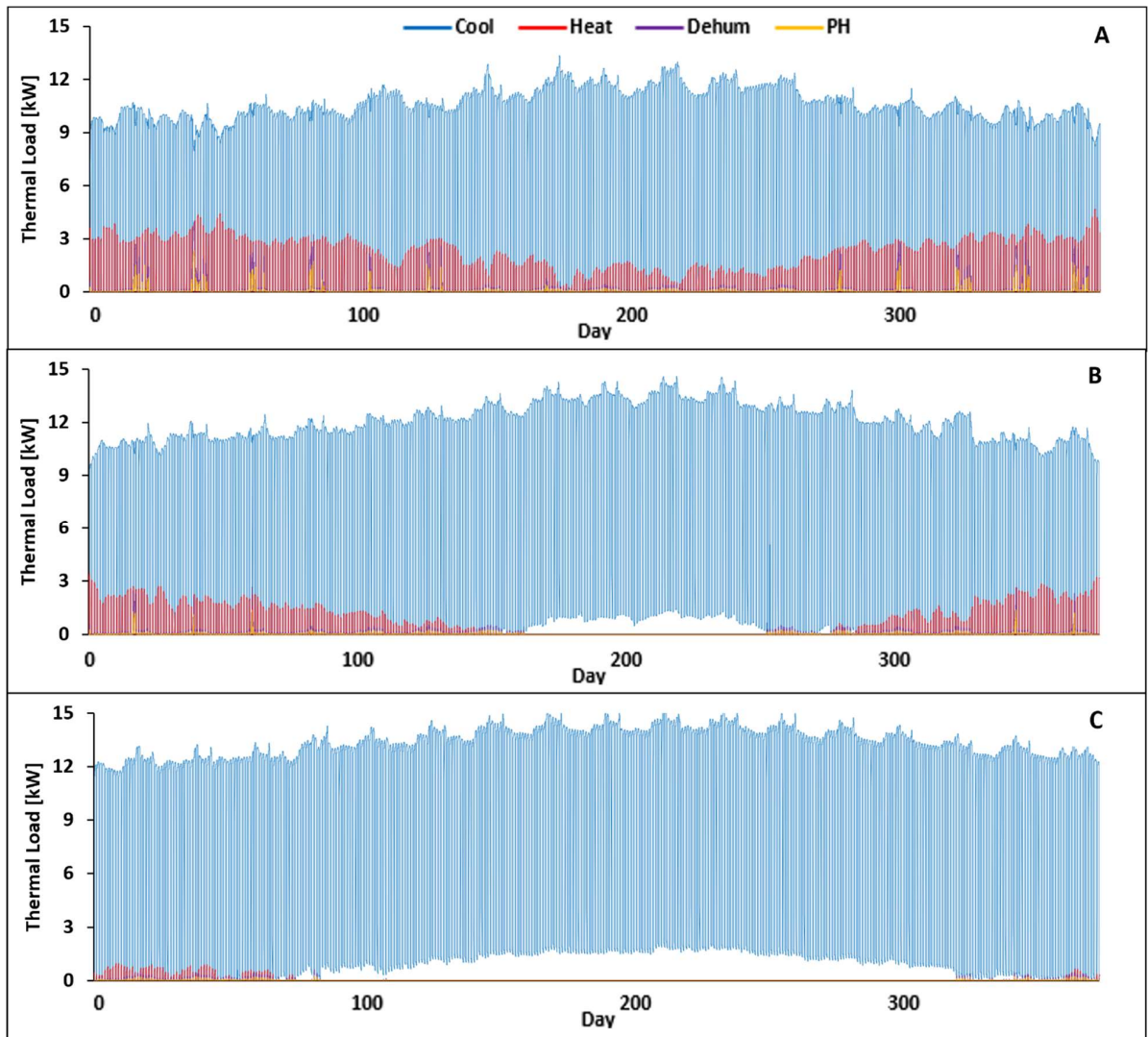


Figure A14: Heating, cooling, dehumidification and post-heating loads throughout the year for a not-insulated VF in three locations: (A) Trondheim, (B) Shanghai, (C) Dubai. The results were obtained under conditions of 20 °C and 400  $\mu\text{mol m}^{-2} \text{s}^{-1}$ .

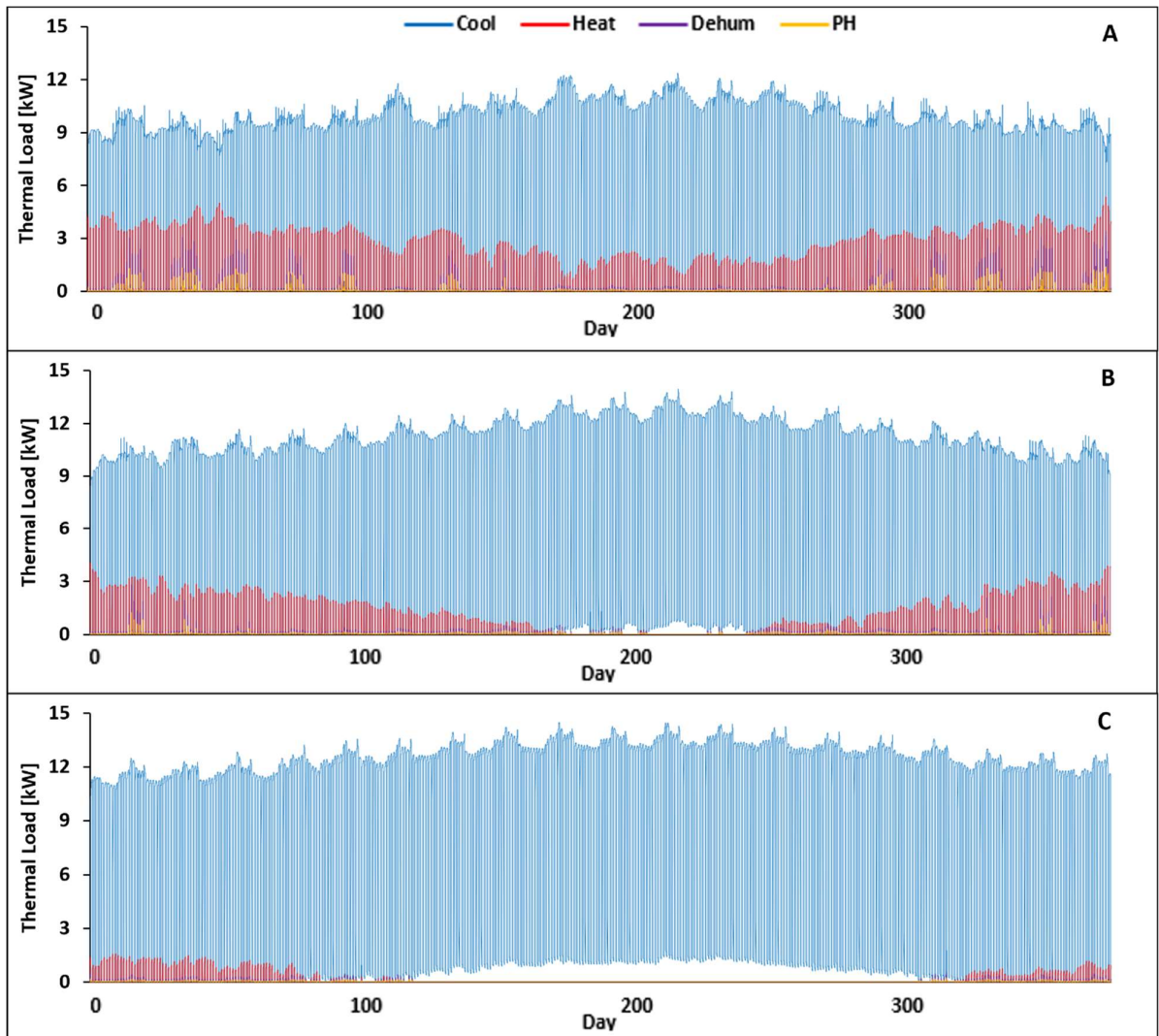


Figure A15: Heating, cooling, dehumidification and post-heating loads throughout the year for a not-insulated VF in three locations: (A) Trondheim, (B) Shanghai, (C) Dubai. The results were obtained under conditions of 24 °C and 400  $\mu\text{mol m}^{-2} \text{s}^{-1}$ .

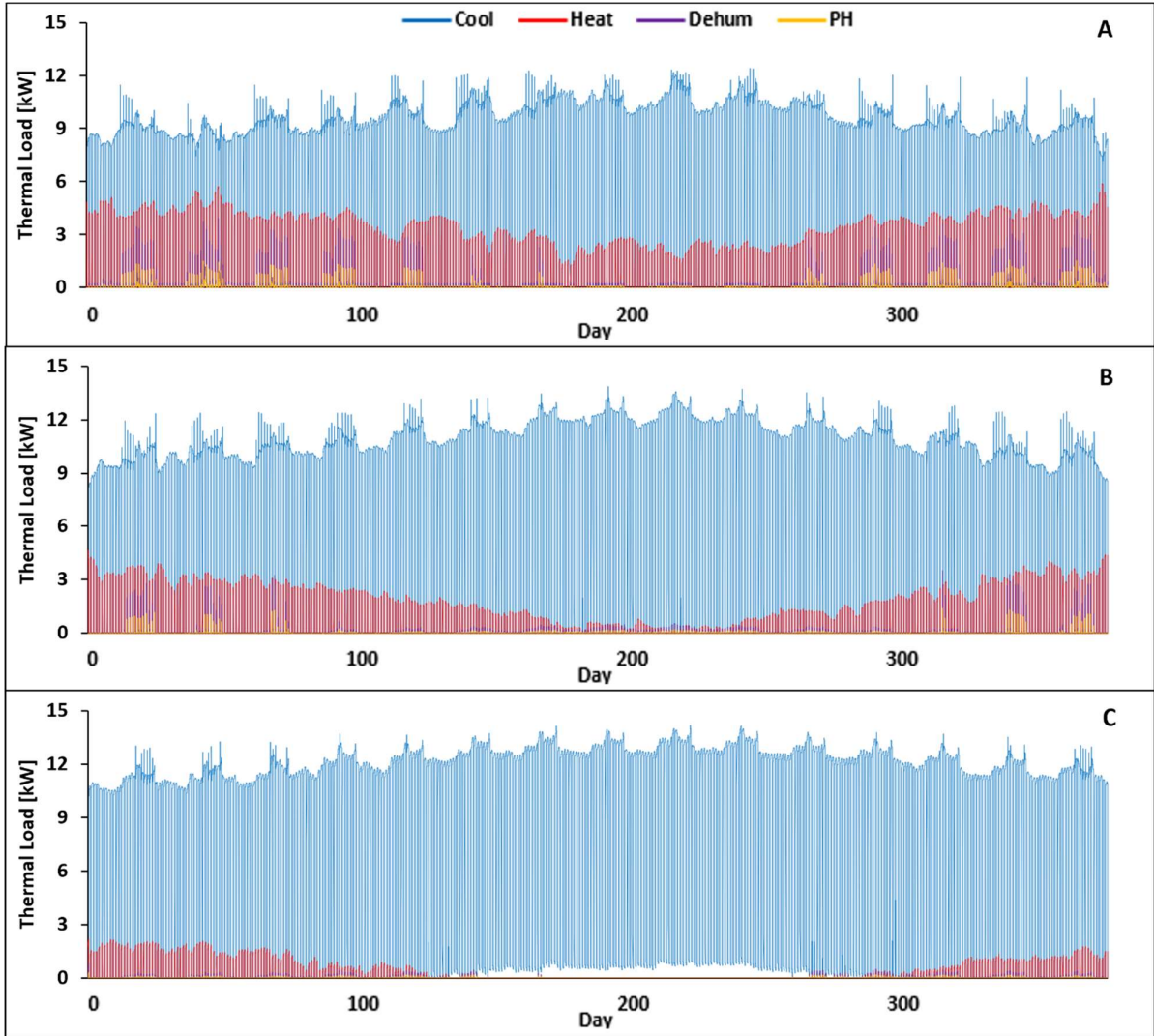


Figure A16: Heating, cooling, dehumidification and post-heating loads throughout the year for a not-insulated VF in three locations: (A) Trondheim, (B) Shanghai, (C) Dubai. The results were obtained under conditions of 28 °C and 400  $\mu\text{mol m}^{-2} \text{s}^{-1}$ .

#### 5.4 Specific Energy Consumption of Not-Insulated Vertical Farm

This section presents the specific energy consumption of the not insulated scenarios. The same assessments discussed in the main body of the paper remain valid for these cases as well. Notably, the absence of an insulation layer leads to an increase in heating demand, particularly in cold climates, which is partially offset by a reduction in cooling load. However, this reduction in cooling increases the VF's dehumidification and post-heating requirements, ultimately resulting in a higher specific energy demand, especially when the PPF is low.

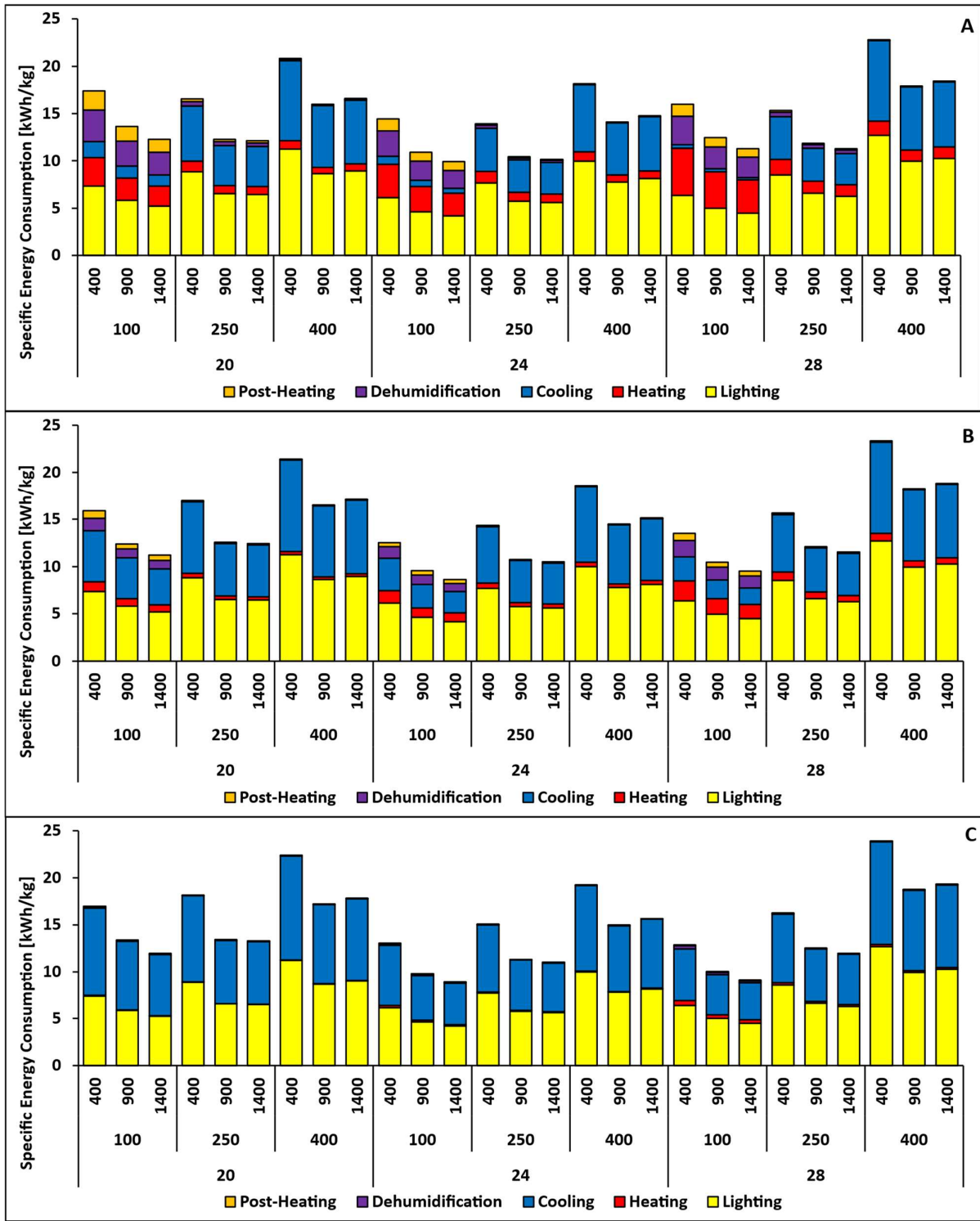


Figure A17: Specific Energy Consumption of the not insulated VF under the three simulated locations: (A) Trondheim, (B) Shanghai, (C) Dubai.

## 6. Declaration of generative AI and AI-assisted technologies in the writing process

During the preparation of this work the authors used ChatGPT 4 in order to improve the readability of the manuscript. After using this tool/service, the authors reviewed and edited the content as needed and take full responsibility for the content of the publication.

## 7. References

- [1] Z. Yu *et al.*, "Energy examination and optimization workflow for container farms: A case study in Shanghai, China," *Appl Energy*, vol. 374, p. 124038, Nov. 2024, doi: 10.1016/j.apenergy.2024.124038.
- [2] A. Dhapte, "Vertical Farming Market Research Report Information By Component (Irrigation Component, Lighting, Sensor, Climate Control, Building Material, Glass Greenhouse, Plastic Greenhouse), By Structure (Building-based Vertical Farms, Container-based Vertical Farms), By Growth Mechanism (Hydroponics, Aeroponics, Aquaponics) And By Region (North America, Europe, Asia-Pacific, And Rest Of The World) -Market Forecast Till 2032," Apr. 2025.
- [3] N. Engler and M. Krarti, "Review of energy efficiency in controlled environment agriculture," *Renewable and Sustainable Energy Reviews*, vol. 141, p. 110786, May 2021, doi: 10.1016/j.rser.2021.110786.
- [4] L. Marcelis, "Vertical farming: Leo Marcelis." Accessed: Apr. 04, 2025. [Online]. Available: <https://www.youtube.com/watch?v=KKbEs5n1HXc>
- [5] W. Jin, D. Formiga Lopez, E. Heuvelink, and L. F. M. Marcelis, "Light use efficiency of lettuce cultivation in vertical farms compared with greenhouse and field," *Food Energy Secur*, vol. 12, no. 1, Jan. 2023, doi: 10.1002/fes3.391.
- [6] L. Carotti *et al.*, "Plant Factories Are Heating Up: Hunting for the Best Combination of Light Intensity, Air Temperature and Root-Zone Temperature in Lettuce Production," *Front Plant Sci*, vol. 11, Jan. 2021, doi: 10.3389/fpls.2020.592171.
- [7] M. S. Ahamed *et al.*, "A critical review on efficient thermal environment controls in indoor vertical farming," *J Clean Prod*, vol. 425, p. 138923, Nov. 2023, doi: 10.1016/j.jclepro.2023.138923.
- [8] P. M. Pattison, J. Y. Tsao, G. C. Brainard, and B. Bugbee, "LEDs for photons, physiology and food," *Nature*, vol. 563, no. 7732, pp. 493–500, Nov. 2018, doi: 10.1038/s41586-018-0706-x.
- [9] M. Cossu, M. T. Tiloca, A. Cossu, P. A. Deligios, T. Pala, and L. Ledda, "Increasing the agricultural sustainability of closed agrivoltaic systems with the integration of vertical farming: A case study on baby-leaf lettuce," *Appl Energy*, vol. 344, p. 121278, Aug. 2023, doi: 10.1016/j.apenergy.2023.121278.
- [10] N. Asgari, U. Jamil, and J. M. Pearce, "Net Zero Agrivoltaic Arrays for Agrotunnel Vertical Growing Systems: Energy Analysis and System Sizing," *Sustainability*, vol. 16, no. 14, p. 6120, Jul. 2024, doi: 10.3390/su16146120.
- [11] M. D'Ostuni, T. Zou, A. Sermarini, and L. Zaffi, "Integrating Greenhouses into Buildings: A Renewed Paradigm for Circular Architecture and Urban Regeneration," *Sustainability*, vol. 16, no. 23, p. 10685, Dec. 2024, doi: 10.3390/su162310685.
- [12] E. A. Velarde Allazo, G. Rondan Sanabria, and J. Mendoza-Montoya, "Systems Review: The Role of Light Spectrum in Plant Productivity and

- Quality in Vertical Farming Systems," in *2023 IEEE XXX International Conference on Electronics, Electrical Engineering and Computing (INTERCON)*, IEEE, Nov. 2023, pp. 1–6. doi: 10.1109/INTERCON59652.2023.10326035.
- [13] F. Moghimi and B. Asiabanzpour, "Economics of Vertical Farming: Quantitative Decision Model and a Case Study for Different Markets in the USA," Sep. 29, 2021. doi: 10.21203/rs.3.rs-943119/v1.
  - [14] A. Arcasi, A. W. Mauro, G. Napoli, F. Tariello, and G. P. Vanoli, "Energy and cost analysis for a crop production in a vertical farm," *Appl Therm Eng*, vol. 239, p. 122129, Feb. 2024, doi: 10.1016/j.applthermaleng.2023.122129.
  - [15] T. Blom, A. Jenkins, R. M. Pulselli, and A. A. J. F. van den Dobbelaer, "The embodied carbon emissions of lettuce production in vertical farming, greenhouse horticulture, and open-field farming in the Netherlands," *J Clean Prod*, vol. 377, p. 134443, Dec. 2022, doi: 10.1016/j.jclepro.2022.134443.
  - [16] F. Ceccanti, G. Di Lorenzo, A. Bischi, L. Incrocci, A. Pardossi, and A. Baccioli, "A transient energy-agriculture model to predict energy footprint of vertical farms," *Energy Convers Manag*, vol. 332, p. 119740, May 2025, doi: 10.1016/j.enconman.2025.119740.
  - [17] M.-H. Talbot and D. Monfet, "Analysing the influence of growing conditions on both energy load and crop yield of a controlled environment agriculture space," *Appl Energy*, vol. 368, p. 123406, Aug. 2024, doi: 10.1016/j.apenergy.2024.123406.
  - [18] A. Farokhi Soofi, S. D. Manshadi, and A. Saucedo, "Farm electrification: A road-map to decarbonize the agriculture sector," *The Electricity Journal*, vol. 35, no. 2, p. 107076, Mar. 2022, doi: 10.1016/j.tej.2022.107076.
  - [19] D. Chen, J. Zhang, Z. Zhang, Y. Lu, H. Zhang, and J. Hu, "A high efficiency CO<sub>2</sub> concentration interval optimization method for lettuce growth," *Science of The Total Environment*, vol. 879, p. 162731, Jun. 2023, doi: 10.1016/j.scitotenv.2023.162731.
  - [20] M. Casanova P, I. Messing, A. Joel, and A. Cañete M, "Methods to Estimate Lettuce Evapotranspiration in Greenhouse Conditions in the Central Zone of Chile," *Chil J Agric Res*, vol. 69, no. 1, Mar. 2009, doi: 10.4067/S0718-58392009000100008.
  - [21] D. J. Connor, R. S. Loomis, and K. G. Cassman, *Crop Ecology Productivity and Management in Agricultural Systems*, 2nd ed. Cambridge University Press, 2011.
  - [22] J. Hirvonen and K. Sirén, "High Latitude Solar Heating Using Photovoltaic Panels, Air-Source Heat Pumps and Borehole Thermal Energy Storage," in *Proceedings of SWC2017/SHC2017*, Freiburg, Germany: International Solar Energy Society, 2017, pp. 1–10. doi: 10.18086/swc.2017.29.06.
  - [23] EU Science Hub, "Photovoltaic Geographical Information System." Accessed: Apr. 17, 2025. [Online]. Available: [https://re.jrc.ec.europa.eu/pvg\\_tools/en/](https://re.jrc.ec.europa.eu/pvg_tools/en/)
  - [24] Johnson Controls, "Johnson Controls Central Plant Optimisation 10 Application Note." Accessed: Apr. 23, 2025. [Online]. Available: <https://docs.johnsoncontrols.com/bas/r/Johnson-Controls/en->

- US/Johnson-Controls-Central-Plant-Optimization-10-Application-Note/Operation-and-troubleshooting/Searching-for-more-efficient-combinations/Upper-and-Lower-Optimal-Percent-Load-reset
- [25] AERMEC, “AERMEC Catalogue,” 2018.
  - [26] J. Eaves and S. Eaves, “Comparing the Profitability of a Greenhouse to a Vertical Farm in Quebec,” *Canadian Journal of Agricultural Economics/Revue canadienne d'agroéconomie*, vol. 66, no. 1, pp. 43–54, Mar. 2018, doi: 10.1111/cjag.12161.
  - [27] TradingEconomics, “United States Consumer Price Index (CPI),” 2025, Accessed: Jul. 17, 2025. [Online]. Available: <https://tradingeconomics.com/united-states/consumer-price-index-cpi>
  - [28] Factory Sale, “PU WALL SANDWICH PANEL”, Accessed: Feb. 19, 2025. [Online]. Available: <https://factory.sale/product/pu-wall-sandwich-panel/>
  - [29] E. Oosterbaan, “Making CO<sub>2</sub> more affordable for vertical farms and greenhouse growers.” Accessed: Apr. 24, 2025. [Online]. Available: <https://www.hortidaily.com/article/9669654/making-co2-more-affordable-for-vertical-farms-and-greenhouse-growers/>
  - [30] Y. Shao, T. Heath, and Y. Zhu, “Developing an Economic Estimation System for Vertical Farms,” *International Journal of Agricultural and Environmental Information Systems*, vol. 7, no. 2, pp. 26–51, Apr. 2016, doi: 10.4018/IJAEIS.2016040102.
  - [31] Water Store, “Refill CO<sub>2</sub> cylinder - 10 kg for rent with H<sub>2</sub>O.” Accessed: Apr. 24, 2025. [Online]. Available: <https://www.h2owaterstore.it/gb/refill-co2-cylinders/4743-refill-co2-cylinder-10-kg-for-rent-with-h2o-7429528783746.html>
  - [32] E. and A. E. China International Gas Technology, “【日评】工业气行情淡稳.” Accessed: Apr. 24, 2025. [Online]. Available: <https://igchina-expo.com/article/item-2307.html>
  - [33] Eurostat, “Electricity prices for non-household consumers - bi-annual data (from 2007 onwards),” Apr. 2025, Accessed: Apr. 24, 2025. [Online]. Available: [https://ec.europa.eu/eurostat/databrowser/view/nrg\\_pc\\_205/default/table?lang=en](https://ec.europa.eu/eurostat/databrowser/view/nrg_pc_205/default/table?lang=en)
  - [34] S. O. I. D. B. Shanghai Foreign Investment Development Board, “Water, electricity and gas,” 2024, Accessed: Apr. 24, 2025. [Online]. Available: <https://english.shanghai.gov.cn/en-EstablishaCompany/20231209/941408eab4d04397ba21064971e9385d.html>
  - [35] Dubai Electricity & Water Authority, “Electricity Tariff,” Jan. 2025, Accessed: Apr. 24, 2025. [Online]. Available: <https://www.dewa.gov.ae/en/consumer/billing/slub-tariff>
  - [36] Trondeheim Kommune, “Vannmåler og priser for vann og avløp,” 2025, Accessed: Apr. 24, 2025. [Online]. Available: <https://www.trondheim.kommune.no/vannmaler/>
  - [37] Economic Research Institute, “Average Hourly Salary,” Apr. 2025, Accessed: Apr. 24, 2025. [Online]. Available: <https://www.salaryexpert.com/salary/job/agronomist/norway>
  - [38] SecondSpace, “Minilager Trondheiim - Tunga.” Accessed: Apr. 24, 2025. [Online]. Available: <https://secondspace.no/minilager-trondheim-tunga>
  - [39] 58App Shanghai, “上海仓库租金走势-日租金.”
  - [40] RedRock Real Estate, “Key Figures and Growth in Q3 2024, Dubai’s Commercial Real Estate Market.” Accessed: Apr. 24, 2025. [Online]. Available: [https://redrockre.ae/insights/key-figures-and-growth-in-q3-2024--dubai%E2%80%99s-commercial-real-estate-market/23?utm\\_source=chatgpt.com](https://redrockre.ae/insights/key-figures-and-growth-in-q3-2024--dubai%E2%80%99s-commercial-real-estate-market/23?utm_source=chatgpt.com)

- [41] M. Martin, M. Elnour, and A. C. Siñol, “Environmental life cycle assessment of a large-scale commercial vertical farm,” *Sustain Prod Consum*, vol. 40, pp. 182–193, Sep. 2023, doi: 10.1016/j.spc.2023.06.020.
- [42] S. Amanda R., “Capital Recovery Costs: An Important Component of Enterprise Budgeting,” *Southern Ag Today*, vol. 3, Oct. 2023, Accessed: May 22, 2025. [Online]. Available: [https://southernagtoday.org/2023/10/11/capital-recovery-costs-an-important-component-of-enterprise-budgeting/?utm\\_source=chatgpt.com](https://southernagtoday.org/2023/10/11/capital-recovery-costs-an-important-component-of-enterprise-budgeting/?utm_source=chatgpt.com)
- [43] Europower, “Norsk strøm har blitt renere.” Accessed: Feb. 14, 2025. [Online]. Available: [https://www.europower.no/forbruker/norsk-strom-har-blitt-renere/2-1-1659019?zephr\\_sso\\_ott=lkdyoF](https://www.europower.no/forbruker/norsk-strom-har-blitt-renere/2-1-1659019?zephr_sso_ott=lkdyoF)
- [44] Ministry of Ecology and Environment of the People’s Republic of China, “关于发布2022年电力二氧化碳排放因子的公告.” Accessed: Apr. 24, 2025. [Online]. Available: [https://www.mee.gov.cn/xxgk2018/xxgk/xxgk01/202412/t20241226\\_1099413.html](https://www.mee.gov.cn/xxgk2018/xxgk/xxgk01/202412/t20241226_1099413.html)
- [45] Dubai Electricity & Water Authority, “DEWA Sustainability Report 2024.” Accessed: Apr. 24, 2025. [Online]. Available: <https://www.dewa.gov.ae/en/consumer/Sustainability/sustainability-reports>
- [46] World Integrated Trade Solution, “Norway Lettuce, fresh or chilled, (excl. cabbage) lettuce imports by country in 2021.” Accessed: Apr. 24, 2025. [Online]. Available: <https://wits.worldbank.org/trade/comtrade/en/country/NOR/year/2021/tradeflow/Imports/partner/ALL/product/070519>
- [47] World Integrated Trade Solution, “Cabbage lettuce, fresh or chilled imports from China in 2023.” Accessed: Apr. 24, 2025. [Online]. Available: <https://wits.worldbank.org/trade/comtrade/en/country/All/year/2023/tradeflow/Imports/partner/CHN/product/070511>
- [48] World Integrated Trade Solution, “United Arab Emirates Lettuce, fresh or chilled, (excl. cabbage lettuce imports by country in 2023.” Accessed: Apr. 24, 2025. [Online]. Available: <https://wits.worldbank.org/trade/comtrade/en/country/ARE/year/2023/tradeflow/Imports/partner/ALL/product/070519>
- [49] S. A. Tassou, G. De-Lille, and Y. T. Ge, “Food transport refrigeration – Approaches to reduce energy consumption and environmental impacts of road transport,” *Appl Therm Eng*, vol. 29, no. 8–9, pp. 1467–1477, Jun. 2009, doi: 10.1016/j.applthermaleng.2008.06.027.
- [50] A. ERGİN and M. F. ERGİN, “Reduction of Ship Based CO<sub>2</sub> Emissions from Container Transportation,” *International Journal of Computational and Experimental Science and Engineering*, vol. 4, no. 3, pp. 1–4, Nov. 2018, doi: 10.22399/ijcesen.429944.
- [51] A. S. van Veghel, S. Sultan, and A. G. Ameryckx, “The carbon footprint of vegetable imports into Aruba: A closer look at sea and air transport,” *Future Foods*, vol. 10, p. 100469, Dec. 2024, doi: 10.1016/j.fufo.2024.100469.